Study on the interfacial mechanism of the supported nickel oxide nanocluster by X-ray absorption fine structure

January 2019

Takuro SASAKI

Department of Applied Chemistry and Biotechnology

Graduate School of Engineering

CHIBA UNIVERSITY

（千葉大学審査学位論文）

Study on the interfacial mechanism of the supported nickel oxide nanocluster by X-ray absorption fine structure

January 2019

Takuro SASAKI

Department of Applied Chemistry and Biotechnology

Graduate School of Engineering

CHIBA UNIVERSITY

（千葉大学審査学位論文）

XAFS による担持ニッケル酸化物ナノクラスターの界面機能に関する研究

2019 年 1 月

千葉大学大学院工学研究科

共生応用化学専攻　共生応用化学コース

佐々木　拓朗

Acknowledgments

This research has been carried out at Department of Applied Chemistry and Biotechnology, Graduate School of Engineering, Chiba University during 2013-2019. I could not write this Ph.D. thesis without the support of many people. I deeply appreciate everyone who has supported me during a doctoral course at Chiba University.

Prof. Nobuyuki Ichikuni, a supervisor, has supported me on everything of my research activity. He responds kindly whenever I ask him a question, and his suggestions are always suggestive and include a clue for the solution. He teaches me a way to conduct research, attitudes for research as a doctoral student, and other various things. During the doctoral course, I obtained many opportunities for attending conferences and research abroad thanks to him. In particular, attending international conferences and research activities in France and Belgium were great experiences, and these experiences surely will make my life wonderful one in the future. Supervision by Prof. Nobuyuki Ichikuni enabled me to spend a great time in the doctoral period. I would like to say my deep gratitude to him.

Prof. Shogo Shimazu advised me particularly at a seminar in Lab. His comments and advises from the various viewpoints led to new insights and success of this work. Besides, I could listen to interesting stories not only about research but also about foreign countries and so on. I would like to appreciate him deeply.

I conversed with Assoc. Prof. Takayoshi Hara particularly during the experiment in the laboratory, and he taught me various things about research. His constructive questions and comments at a seminar made my research greater. I greatly appreciate his help with everything.

Ms. Yoshiko Ichihara, secretary, supported mainly about office procedure. I would like to thank her for her help.

I also would like to appreciate Prof. Naofumi Uekawa, Prof. Nagahiro Hoshi, Prof. Takashi Mino, Prof. Nobuyuki Ichikuni, Prof. Shogo Shimazu, and Assoc. Prof. Takayoshi Hara. They undertook a judgment of my Ph.D. thesis and gave me a lot of valuable comments and advises. I could brush up my thesis thanks to them. I am sure that this experience of Ph.D. defense

will contribute to my good work in the future.

Prof. Eric M. Gaigneaux, Dr. François Devred, Dr. Pierre Eloy, and Ms. Françoise Somers (secretary) accepted and supported me on research at Université catholique de Louvain. XPS and in situ XRD measurements were carried out there, and I could write a paper as a collaborated work. I appreciate them for everything during the stay.

I could short-study abroad not only in Belgium but also in France, and Prof. Didier Sebilleau and Assoc. Prof. Keisuke Hatada accepted and supported me on the study at Université Rennes 1, France. I studied physics and calculation of X-ray scattering, and I could expand my insights. This studying abroad was a good opportunity to think of having a job internationally. I would like to appreciate them greatly.

Research activities in Belgium and France were achieved by the support of Prof. Peter Krüger and Ms. Yuri Shinozuka (secretary). I am greatly happy to obtain the wonderful opportunities to research in foreign countries. I would like to appreciate them. In addition, these activities were granted from JASSO.

Assoc. Prof. Kiyotaka Nakajima helped me with measuring and analysis of TEM. I would like to appreciate his kind support.

Attending the international conference was achieved by a grant from Chiba University SEEDS fund. I would like to appreciate contributors to the fund.

I would like to say my gratitude to all of the students and friends who research together in Lab. 12. Going for lunch, having a drink, and talking with them enabled me to have a fulfilling research life. I greatly appreciate them.

I have caused my parents anxiety, but they support and encourage me every time. I could not write this thesis without them. I would like to show my maximum gratitude to them.

January, 2019 Takuro SASAKI

Contents

Chapter 1

General Introduction

1.1. Development of catalyst concerning the sustainable society

1.1.1. Heterogeneous catalyst

The catalyst is a substance which can make the activation energy lower, promote the reaction rate, and create the new reaction path. The catalyst has been investigated and it has contributed to the development of society, industry, and academic field [1].

The catalyst is classified roughly into the homogeneous catalyst and heterogeneous catalyst. When the phases of a catalyst and a reactant are the same, the catalyst is called as a homogeneous catalyst. On the other hand, if the phases are different it is called as a heterogeneous catalyst. In many cases of homogeneous catalysts, both the catalyst and reactant are liquid phase, and those of heterogeneous catalyst, the catalyst is solid state and reactant is liquid or gas phase [1].

There are some advantages and disadvantages regarding those two types of the catalysts. The homogeneous catalyst is favorable in terms of activity and selectivity compared to the heterogeneous catalyst. In particular, the selectivity of homogeneous catalyst is excellent and the homogeneous catalyst is expected to play an important role for the production of fine chemicals, pharmaceutical products, and functional polymer. However, the homogeneous catalyst has a disadvantage as well, and the separation of the catalyst and reactant is complicated.

On the other hand, the heterogeneous catalysts can be easily separated from reactant by simple ways such as the centrifugation and filtration. The heterogeneous catalyst is desirable because of the reusability concerning the achievement of sustainable society. The development of the heterogeneous catalyst possessing high activity and selectivity is an ideal approach in modern society where the environmentally friendly development is one of the most important keywords.

As heterogeneous catalysis have evolved, it has become more apparent that it has a large part to play in green chemistry and thus removing or substantially reducing pollution and undesirable by-products from both the chemical and refining processes [2-4]. In the other words, the by-products of heterogeneous catalyst reactions would not end up with harmful emissions and

nasty waste materials that are dangerous and detrimental to the ecosystems and the environment [3].

1.1.2. Precious metal substituting catalyst

Until today, many kinds of heterogeneous precious metal catalysts have been developed as a useful catalyst. The precious metal catalysts are prepared by using the precious metal such as Ru [5-7], Rh [8-10], Pd [11-13], Pt [14-16], Au [17-19], and so on. The precious metal catalysts show the high catalytic activity and good corrosion resistance, and these catalysts showed great performance for the hydrogenation of arenes [6,8,14] and alkynes [13,18], the CO methanation [7], the hydroformylation of butane [10], the Suzuki-Miyaura coupling reaction [11], the oxidation of formaldehyde [15], the CO oxidation [17], and so on. In addition, they have good reusability, and they are useful as a heterogeneous catalyst utilizing its advantage which homogeneous catalysts do not have.

However, the abundance of the precious metal is not much (Fig. 1.1 [20]), and there is a concern about the resource shortage. Hence, the development of precious metal substituting catalyst using the base metal such as Mn, Fe, Co, Ni, Cu, and so on is strongly desired in terms of the sustainable society.

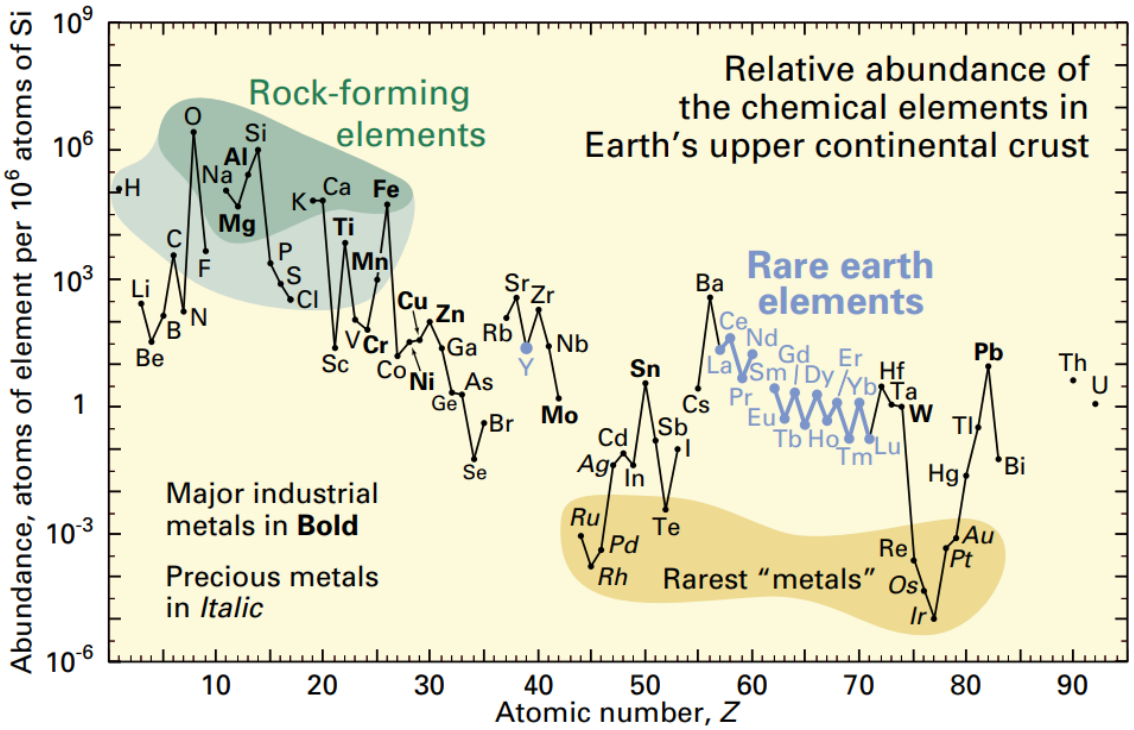

Fig. 1.1. Abundance (expressed as atoms of element per 106 atoms of Si) of the chemical elements in Earth's upper continental crust as a function of atomic number. Many of the elements are classified into the following (partially overlapping) categories: (1) rock-forming elements (major elements in green field and minor elements in light green field); (2) rare earth elements (lanthanides, La-Lu, and Y; labeled in blue); (3) major industrial metals (global production >B3 107 kg per year; labeled in bold); (4) precious metals (italic); and (5) the nine rarest "metals"-the six platinum group elements plus Au, Re, and Te (a metalloid). Reproduced with permission from U.S. Geological Survey, Department of the Interior. Fig. 1.1 is adapted from ref. [20] Accessed from website http://pubs.usgs.gov/fs/2002/fs087-02/

1.1.3. Nickel catalyst

In this work, nickel was focused on as an active species. Nickel, the first row transition metal, is more abundant compared to the precious metals as shown in Fig. 1.1. Besides, nickel is expected to be used as a catalytic material, and nickel is one of the candidates for the objective, the achievement of sustainable society.

The representative nickel catalyst, Raney nickel, and the other various types of nickel metal catalysts show catalytic activity to various reactions such as the hydrogenation of alkenes, nitroarenes, and aromatic compounds [21-30] (e.g. Raney Ni [21-23], Ni/AC_{OX} [25], Ni/clay [30]), the CO_2 dry reforming of methane [31-40] (e.g. Ni/SiO_2 [31], Ni/γ-Al_2O_3 [32], Ni/SBA-15 [33]), the steam reforming of ethanol [41-50] (e.g. Ni/Al_2O_3 [41], Ni/SiO_2 [42], Ni/CeO_2 [43]), and the glycerol steam reforming [51-60] (e.g. Ni/CeO_2 [51], Ni/ZrO_2 [52], Ni/γ-Al_2O_3 [53,55,56]). As mentioned above, nickel metal catalysts are used and investigated in the various fields.

On the other hand, oxidized nickel such as NiO and $Ni(OH)_2$ are used mainly for the electrode catalysts or semiconductor [61-70]. NiO is used as a catalyst also for the CO oxidation [71], dehydrogenation of ethane and toluene [72,73]. However, CO oxidation and dehydrogenation of ethane are the reaction using light gas molecular as a reactant, and the oxidation of toluene needs the high temperature (772 K). These facts means that there are much less research report which the oxidized nickel is an active species for the organic reactions in the fine chemicals field compared to the nickel metal catalysts.

Some research reported that the oxidized nickel (NiO_2 and $Ni(OH)_2$) showed activity to the oxidation of alcohols which is one of the fine chemical reactions, however S/C ratio is 0.31 and 0.30, respectively, and the excess amount of nickel was used for the reaction [74,75]. Besides, the composite material, Ni-incorporated hydrotalcite, was utilized for the oxidation of alcohols [76,77], TON is still 1.6 and 0.7, respectively. There is the room to improve the catalytic activity of the oxidized nickel catalyst, and research on these catalyst is still insufficient. Therefore, application of and research on the oxidized nickel catalysts for the oxidation of alcohols are the crucial issue in terms of the expansion of new application and of the elementary strategy.

In many cases, nickel is used for the hydrogenation reaction or steam reforming reaction,

and it is not general to be used for the oxidation of aromatic compounds. However, we have already found that SiO_2 supported NiO catalyst is active to the oxidative coupling of thiophenol. Considering from that result, NiO catalyst is expected to be active to another oxidative reaction such as oxidation of alcohols. Regarding the expansion of science of the nickel catalyst, the oxidation of alcohols was focused on in this work.

1.2. Oxidation of alcohols

The aerobic oxidation of alcohols to their corresponding aldehydes or ketones is one of most important processes in industry and academia [78-80]. Aldehydes and ketones produced from the oxidation reactions are applied as an intermediate of medical drugs, agricultural chemicals or aroma chemicals [81,82].

Traditional methods to accomplish this transformation rely on the stoichiometric amount of metallic or organic oxides, which are expensive, toxic and tend to generate large amounts of hazardous waste [83]. To overcome these inherent problems, significant efforts have been devoted to developing catalytic oxidation alternatives using molecular oxygen as the terminal oxidant during the past decade [78,84,85]. On the other hand, various catalysts having the activity to the oxidation of alcohols using molecular oxygen as an oxidant have been developed, however some of them need the external base such as NaOH, K_2CO_3, Cs_2CO_3, or KOH [86-89]. These additives and conditions will cause the problem of complicated purification and pollution. Thus, considering the aerobic oxidation of alcohols, a clean catalytic process, where ambient molecular oxygen is used as an oxidant instead of high-pressured oxygen or TBHP which are more harmful and the addition of external bases is not needed, is desired in terms of green chemistry.

Heterogeneous nickel-based catalysts have been prepared for the aerobic oxidation of alcohols using molecular oxygen as an oxidant without any base additives [74-77] as mentioned in section 1.1.3. However, excess amount of nickel to substrate was used (Substrate/$Catalyst_{Ni}$ mol ratio (S/C ratio) = 3.1 [74], 0.45 [75], 0.31 [76], 0.30 [77) for the catalysis and there is the room to improve the catalytic efficiency (TON = 1.6 [74], 0.45 [75], 0.30 [76], 0.24 [77]). Highly functional heterogeneous nickel catalyst needs to be prepared to improve the activity and

efficiency, and the application of nanocluster and support is expected to be a way of the high-functionalization.

1.3. Approach for the highly functional nickel catalyst

1.3.1. Application of nanocluster

The conventional nickel-based catalysts mentioned in previous section are bulk catalysts, and the application of nanocluster are expected to be a useful way to improve the catalytic performance due to its nanosized effect as well as high specific surface area.

The atom aggregate which is composed of at most a few hundred atoms is called as the nanocluster. The property of nanocluster is definitely different from that of the bulk. The nanocluster shows a unique engineering, magnetic, mechanic, and chemical property [90]. These properties originate from the increase of the number of surface atoms, and the nanocluster is applied in the wide range of fields such as the field of engineering and medical science. In addition, because the number of surface atoms depends on the cluster size, the fundamental research on the microminiaturization has been conducted actively [91-96].

The nanocluster is gathering much attention as a unique catalyst material due to the nanosized effect as well as its high atom efficiency, and hence, they are investigated also in the field of catalyst chemistry. Since the development of the active gold nanocluster by Haruta et al. [97], research on nanocluster catalysis has become more popular. The fact that they were able to apply Au to the catalytic reaction was a big impact because Au has been regarded as an inactive element as a catalyst. Furthermore, this Haruta's success implied that other elements also can have a potential to show the catalytic activity.

We also have investigated nanocluster catalysts using nickel as an active species. We have found the appearance of catalytic activity caused from nanoclusterization and the dependency on cluster size for WGSR [98,99] and oxidative coupling of thiophenol [100,101].

Effects of nickel oxide on activity have been reported [102,103]. The nanoclusterization, an increase of the coordination unsaturated sites, enables the localization of electron density on the unsaturated Ni-O site [102], resulting in the high Lewis acidity of the Ni atom, facilitating the cleavage of O-H bond of alcohols, and promoting the elimination of α-hydride (H^-) of alcohols [103]. Thus, the nickel oxide nanocluster is expected to be active to the oxidation of alcohols as illustrated in Scheme 1.1. This electronic localization does not occur on Ni metal between two atoms in a metal in contrast to NiO. Also in terms of this fact, it is considerably interesting to research on NiO catalysis.

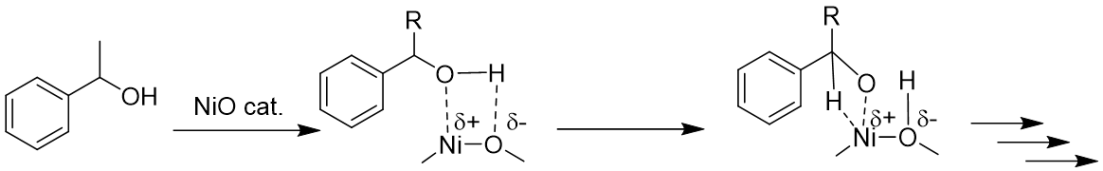

Scheme 1.1. Mechanism for the oxidation of alcohols by nano-sized nickel oxide.

1.3.2. Application of support

We also focused on the application of support as the way to prepare the high-performance catalyst. Heterogeneous catalysts have been investigated actively in terms of the achievement of sustainable society as mentioned in section 1.1.1. Herein, the support can role some important roles for the heterogeneous catalysts. For instance, support such as metal oxides, carbon, and zeolite is often used as a foundation to prepare the heterogeneous catalyst [104-109]. Catalysts generate the profit for various production fields such as pesticides [110], polymers [111,112], antibiotics [113,114], cosmetics [115], cleaning products [116] and so on. Catalysts utilized frequently in the industrial field is heterogeneous catalysts which metals as an active species is fixed on support. Until today, various kinds of supported catalysts have been developed aiming at the achievement of high activity and selectivity.

Catalysis is affected by the catalyst structure including surface atomic arrangement and coordination, which can be controlled by regulating the composition, morphology and size of active species [114-117]. Regarding the supported catalysts, catalytically active species is fixed

on a support possessing large surface area such as silica, alumina, zeolite and so on. Support is utilized to stabilize high dispersion of active species such as noble metal nanoparticles and to prevent from sintering.

To heterogenize homogeneous catalysts by using support is often desired in the field of industrial chemical engineering [118]. For easier separation of a catalyst from the fluid products and reactants, the heterogeneous catalysts are desired. Also, utilizing heterogeneous catalysts enable packing catalysts inside a reactor in the production process of chemicals. In addition, to avoid the aggregation of active species, particularly nano-sized particles, is one of the most important reasons to utilize a support material [3,119]. However, week interaction between the nano-sized active species and support surface still causes the aggregation [120]. Strongly attaching the nano-sized active species to the support surface as a heterogeneous catalyst results in the creation of defect sites on the surface or functional group bonding to the surface, which can make catalysts to be more active [121-123]. Based on the above idea, researchers have studied on many kinds of support materials such as silica, carbon, zeolite and so on [124].

Regarding the nickel catalysts, research on the structural analysis and catalysis of SiO_2 [100,101,125], Al_2O_3 [98,99,126], or MgO [127-129] supported nickel catalysts has been reported. Mesoporous support was also used as a support for the nickel catalyst [130-132]. It was reported that mesoporous alumina possessing the three dimensional mesoporous structure can prevent the aggregation of nickel particles, resulting in the high dispersion and activity. In other words, the fixing onto the support can facilitate the synthesis of nanocluster, resulting in the high-performance catalyst.

Besides the stabilization and dispersion of the active species, another effect is expect to contribute to the high-performance catalysts. Catalyst supports can promote a catalytic reaction and/or result in the new active site as an interfacial structure as well as stabilize the active species on its surface. Haruta *et al.* reported that the reason why the Au nanocluster catalyst showed the activity to CO oxidation even at 203 K was that the interfacial structure between Au nanocluster and support was able to activate molecular oxygen. They also described that the reaction rate of CO oxidation was in proportion to the length of perimeter [17].

As mentioned above, the effective contribution of interfacial structure between the active species and support to the catalytic reactions is essential factor to design a highly active

catalyst. The utilizing nanocluster can enhance that contribution due to the increase of interfacial area as well as cause its unique surface property since the unsaturated site. The understanding the interfacial structure and mechanism is also crucial issue to design the high-performance catalysts. The expansion of new guideline of the catalyst design can result from the understanding a role of the interfacial structure between active species and support.

1.4. Characterization of catalyst

Various techniques are used to characterize the catalyst structure in order to clarify the correlation between catalyst structure and catalytic activity, or the origin of catalysis including the interfacial structure. Clarifying the origin of catalysis can lead to the expansion of guideline of catalyst design. We particularly focused on the application of X-ray absorption fine structure (XAFS) as a means of the characterization of catalyst. The feature of the XAFS was described below [133];

The structure of the nanocluster catalyst which does not have a long-range ordered structure cannot be examined by X-ray diffraction measurement. However, the characterization via XAFS does not need the long-range ordered structure of the nanocluster catalysts.

Regarding XAFS, X-ray used to excite the inner shell electron is measured as an absorption coefficient. When the absorption coefficients of materials are measured changing the X-ray energy, a sudden increase of absorption can be detected at a certain level of energy, known as the absorption edge.

The spectrum on near region of the absorption edge is called as X-ray absorption near edge structure (XANES). The XANES shape is sensitive to the number of atoms bonding to the target element, symmetry, type of ligand or element, and valence state.

The extended X-ray absorption fine structure (EXAFS) appears as periodic changes of absorption on the high-energy side of the absorption edge. The periodic changes can be explained as the interference of the electron waves. The electron wave released from the X-ray absorbing atom is scattered by the surrounding atoms, returns to the X-ray absorbing atom and interferes

with the original electron waves. The EXAFS noted as a new structure analyzing method leads us to useful information about structural parameters such as coordination number, interatomic distance, and symmetry around the atom. The XAFS is one of the most promising techniques for the structural analysis of highly dispersed metal species in catalyst.

As mentioned above, the interface structure between the active species and support can contribute to the appearance of catalytic activity. Therefore, the interfacial structure is one of the key factors and its characterization is a crucial topic. In this work, the interfacial structure and its mechanism against the catalysis as well as the surface chemical species and support was characterized by utilizing XAFS and the other characterization techniques.

Chapter 2

General Experimental

2.1. Materials

Nickel nitrate hexahydrate ($Ni(NO_3)_2 \cdot 6H_2O$), ammonia aqueous solution (28.0-30.0%), activated carbon (powder, neutral), sodium silicate (Sodium oxide (Na_2O) 17.0-23.0%, silicon dioxide (SiO_2) 51.0-61.0%, molar ratio (SiO_2/Na_2O) 2.00-3.50), nickel chloride (anhydrate), hydrochloric acid, Polyvinylpyrrolidone (PVP, K30), Hydrotalcite (HT), Magnesium oxide (MgO), benzyl alcohol, 1-phenylethanol, biphenyl, Tetrahydrofuran (THF, super dehydrated, stabilizer free), *t*-Butanol (*t*-BuOH), Sodium borohydride ($NaBH_4$), toluene, and *p*-xylene were purchased from FUJIFILM Wako Pure Chemical Co., Ltd. Nickel acetylacetonate dihydrate was purchased from Kanto Chemical Co., Inc. Silica (SiO_2; Aerosil#200) and alumina (Al_2O_3; Al_2O_3-C) were provided from Nippon Aerosil Co., Ltd.

2.2. Catalyst preparation

In this work, two catalyst preparation methods, impregnation method and liquid phase reduction method, were utilized to prepare the supported nickel oxide nanocluster catalysts.

Impregnation is one of the most common methods. In this method, active species can be fixed on the support surface by dry and calcination after catalyst component is impregnated on the support powder. The kind of active species and cluster size of nickel oxide was controlled by using different nickel precursor and calcination at different temperature in this work.

Liquid phase reduction method is known as one of the methods to prepare a nanocluster catalyst [134], and nano-colloid is used as a precursor. Reduction of nickel salt or complex in solvent with a stabilizer such as alkoxide, polymer, or surfactant can produce the size-regulated nickel nano-colloid. Supported nickel oxide nanocluster catalyst is obtained by fixing nickel nano-colloid on the support followed by the oxidation in air at room temperature.

2.3. Characterization of catalysts

XAFS, TEM, XPS, and *in-situ* XRD were carried out to characterize the prepared catalysts.

Ni *K*-edge XAFS (X-ray absorption fine structure) data were collected at BL-9C of KEK-PF (Proposal No. 2014G575 and 2016G069) with Si(111) double crystal monochromator in a transmission mode at room temperature. XAFS data were analyzed by the analysis software, REX2000 (Rigaku Corp.) TEM images were obtained by JEM-2100F with an accelerating voltage of 200 kV.

XPS measurement was carried out on an SSX 100/206 photoelectron spectrometer from Surface Science Instruments (USA) equipped with a monochromatized micro-focused Al X-ray source (powered at 20 mA and 10 kV). The C-(C, H) component of the C1s peak of carbon has been fixed to 284.8 eV to set the binding energy scale. Data treatment was performed with the CasaXPS program (Casa Software Ltd, UK).

In situ XRD experiments were carried out on a D8 Advanced diffractometer from Bruker with a Bragg Brentano geometry. A Paar Instrument XRK 900 chamber was used to control the reducing atmosphere (30 $mL \cdot min^{-1}$ of 10% H_2 in Helium) and the temperature (from room temperature to 723 K). Each diffraction pattern was recorded using a linkeye XE-T detector (Bruker) in the appropriate 2θ range (from 40 to 50 degrees in 2θ, the increment of 0.02 degree and integration time of 0.3 s).

2.4. Catalytic reaction

Oxidation of 1-phenylethanol or benzyl alcohol was carried out as a catalytic reaction to evaluate the catalytic activity and to understand the catalysis of prepared catalysts.

Oxidation of 1-phenylethanol and benzyl alcohol was carried out as follows: 1-phenylethanol (1 mmol) or benzyl alcohol (1 mmol), and *p*-xylene (5 mL) or toluene (5 mL) were

stirred in Schlenk tube with the catalyst (S/C ratio: 12). Yield of acetophenone or benzaldehyde was determined by gas chromatography (Shimadzu, GC-2025) with capillary column (Hewlett Packard, Ultra 2, 25 m x 0.20 mm, 0.33 μm or GL Science, TC-WAX, 30 m x 0.25 mm, 0.50 μm) and FID detector. Biphenyl (0.5 mmol) was used as an internal standard. Reaction temperature, reaction time, and atmosphere were varied to interpret the catalytic mechanism and catalysis.

Chapter 3

Creation and effect of Ni-O-Si interfacial structure

3.1. Introduction

There are various ways to prepare the supported catalysts, such as sol-gel method [135], ion exchange method [136], deposition-precipitation method [137], and colloidal method [138]. Cluster size and catalyst structure are important factors to design the supported catalysts [17,99].

Regarding colloidal method, different precursor can differ the particle size [100]. Hence, it can be said that cluster size is controlled by also impregnation method, which is one of the easiest ways to prepare the supported catalyst, using various precursor. Changing the precursor can control the cluster size.

In this chapter, the correlation of catalytic activity and structure is discussed from the viewpoint of cluster size and interfacial structure.

3.2. Experimental

In this chapter, catalysts were prepared by impregnation method. NiO(amm)/SiO_2-*T*, NiO(amm)/AC-*T*, NiO(ace)/SiO_2-*T* and NiO(nit)/SiO_2-*T* were obtained by impregnating $[Ni(NH_3)_6]^{2+}$, $Ni(acac)_2$ or $Ni(NO_3)_2$ on SiO_2 (Fuji Silysia, CARiACT P-10) or activated carbon (denoted as AC), followed by calcination at *T* (K) in air. Precursors are abbreviated as *amm*, *ace* and *nit* for $[Ni(NH_3)_6]^{2+}$, $Ni(acac)_2$ and $Ni(NO_3)_2$, respectively. Loading amount of NiO was regulated to 5 wt%.

XAFS and TEM measurement were carried out to characterize the prepared catalysts. Catalytic activity was evaluated by oxidation of 1-phenylethanol.

3.3. Results and discussion

3.3.1. XAFS measurements

Fig. 3.1 shows a Ni *K*-edge XANES (X-ray absorption near edge structure) of prepared NiO catalysts and reference compounds. Information about valence and chemical states of nickel species of the catalysts can be obtained from the XANES spectra. Based on the XANES shape and edge position, all catalysts was consisted of not Ni metal but nickel oxide. However, a slight difference was observed in the white line region. The peak top of white line of NiO(amm)/SiO_2-*T* was at higher energy position than that of NiO(nit)/SiO_2-673, NiO(ace)/SiO_2-673 and NiO(amm)/AC-573, which indicates that a kind of nickel species of each catalyst was different. Energy position of white line of nickel silicate synthesized by reported method [139] was at near position of NiO(amm)/SiO_2-*T*. This result shows the interfacial structure of NiO(amm)/SiO_2-*T*, Ni-O-Si structure, existed besides nickel oxide.

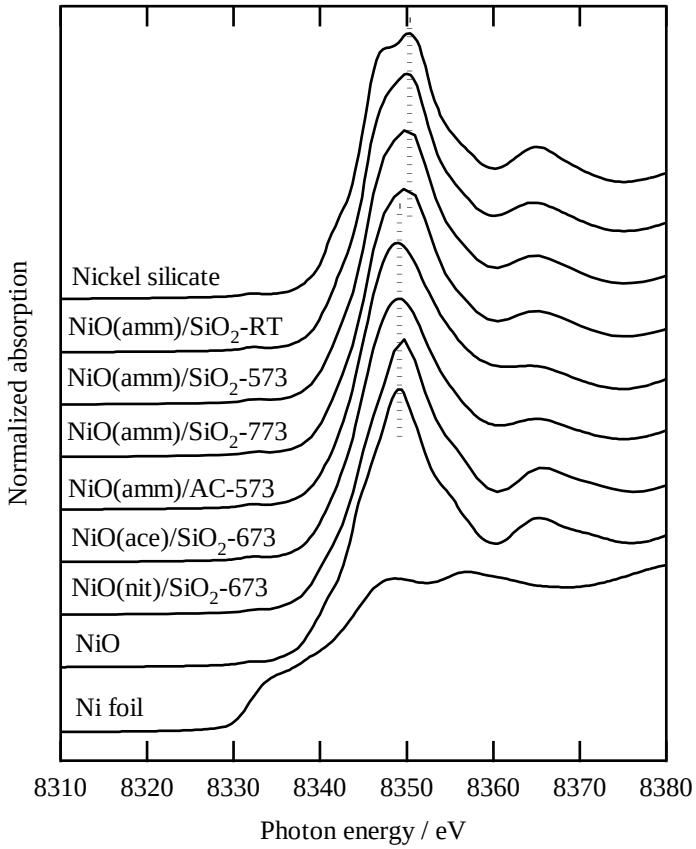

Fig. 3.1. Ni *K*-edge XANES of prepared catalysts and reference compounds.

To obtain the information about local structure in detail k^3-weighted EXAFS (Extended X-ray absorption fine structure) was analyzed. The k^3-weighted EXAFS functions and their Fourier transformed spectra (FT) of prepared catalysts and reference compounds are shown in Fig. 3.2 and Fig. 3.3, respectively. Curve fitting analysis of EXAFS oscillation was carried out for the nearest Ni-Ni coordination by using NiO as a reference compound at around 0.28 nm in FT. Results of the curve fitting analysis is shown in Table 3.1.

EXAFS oscillation patterns of NiO(nit)/SiO_2-673, NiO(ace)/SiO_2-673 and NiO(amm)/AC-573 were same as that of NiO although their amplitudes were different, which indicates that nickel species of these catalysts were NiO as with the result of XANES. Also it is can be said that the kind of nickel species was same but the cluster size was different among them. In fact, coordination number (*CN*) of the nearest Ni-Ni coordination for NiO(nit)/SiO_2-673, NiO(ace)/SiO_2-673 and NiO(amm)/AC-573 was determined to 12.3, 7.0 and 5.0, respectively,

which indicated the different size of NiO particle, and this result resulted from different precursor and support.

On the other hand, the oscillation of NiO(amm)/SiO_2-*T* were different from NiO and similar to that of nickel silicate, which means that Ni-O-Si structure existed as another nickel species on NiO(amm)/SiO_2-*T*. This result agreed with the result of XANES as shown in Fig. 3.1. In addition, *CN* of NiO(amm)/SiO_2-*T* (*CN*=7.3, 7.4, 8.0) was smaller than NiO (*CN*=12), probably meaning the fixing of NiO nanocluster on the support.

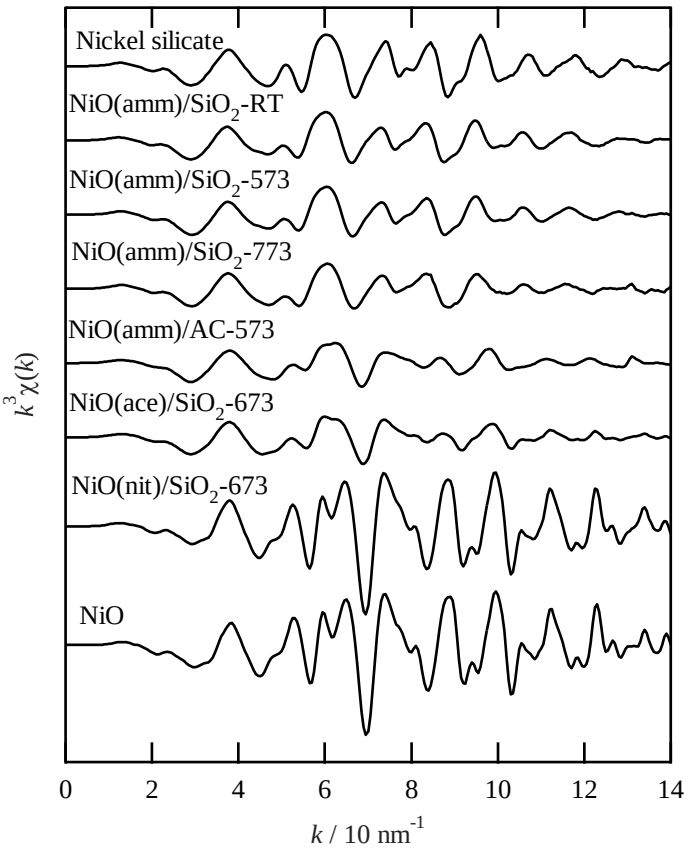

Fig. 3.2. k^3-Weighted EXAFS of prepared catalysts and reference compounds.

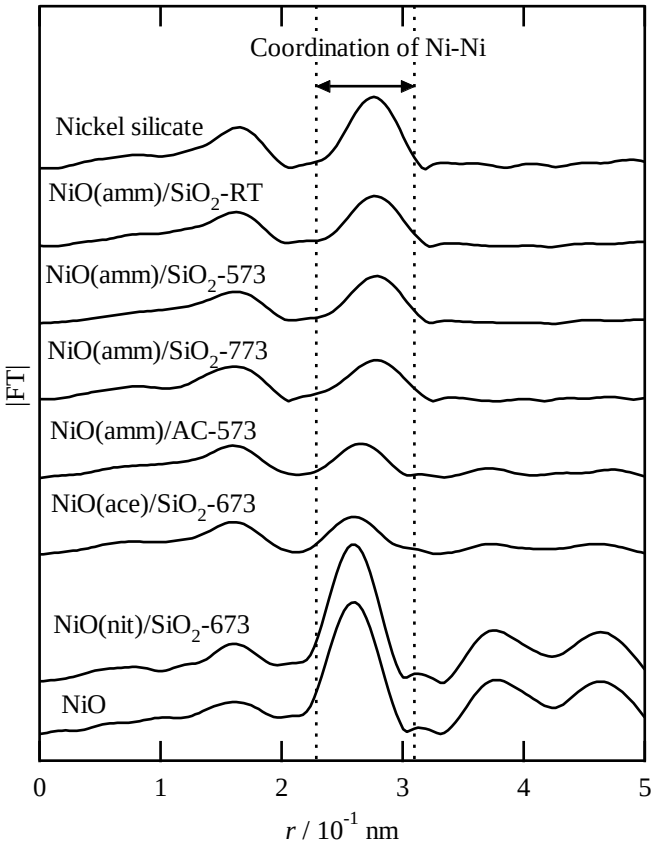

Fig. 3.3. FT of Ni *K*-edge EXAFS for NiO catalysts and reference compounds.

Table 3.1 Curve fitting analysis of FT for the nearest Ni-Ni coordination of NiO catalysts

Catalyst	CN^a	r^b (nm)	dE^c (eV)	DW^d (nm)	R^e
nickel silicate	6	0.307	0	0.006	-
NiO(amm)/SiO_2-298	7.3±1.2	0.311±0.001	4.5±1.6	0.0073	0.012
NiO(amm)/SiO_2-573	7.4±1.2	0.311±0.001	4.8±1.5	0.0079	0.026
NiO(amm)/SiO_2-773	8.0±1.3	0.310±0.001	5.3±1.5	0.0090	0.171
NiO(amm)/AC-573	5.0±0.8	0.300±0.001	1.2±1.5	0.0083	0.132
NiO(ace)/SiO_2-673	7.0±1.2	0.298±0.001	-1.9±1.6	0.0095	0.377
NiO(nit)/SiO_2-673	12.3±2.1	0.295±0.001	0.5±1.7	0.0060	0.090
NiO	12	0.295	0	0.006	-

[a]Coordination number, [b]bond distance, [c]difference between model compound and experimental threshold energies, [d]Debye-Waller factor, [e]R-factor. FT range: 30-140 nm^{-1}.

Regarding the formation of Ni-O-Si structure, a reaction between nickel precursor and SiO_2 during catalyst preparation was considered. NiO(amm)/SiO_2-*T* was prepared under basic condition by using ammonia solution to utilize $[Ni(NH_3)_6]^{2+}$ as a nickel precursor. A part of the SiO_2 framework dissolves under basic condition and new silanol group forms [140]. Subsequently, it is assumed that nickel species penetrated the SiO_2 framework and Ni-O-Si bond forms on the new silanol group. A formation of nickel silicate was reported regarding a SiO_2 supported catalysts synthesized from $[Ni(NH_3)_6]^{2+}$, nickel precursor [141, 142].

Nickel species penetrating the silica frame work can be Ni-O-Si structure, and nickel species which did not go into the framework seemed to be supported on Ni-O-Si structure as NiO. Therefore, Ni-O-Si structure is an interfacial one, and NiO and Ni-O-Si structure coexisted across the SiO_2 surface as shown in Fig. 3.4.

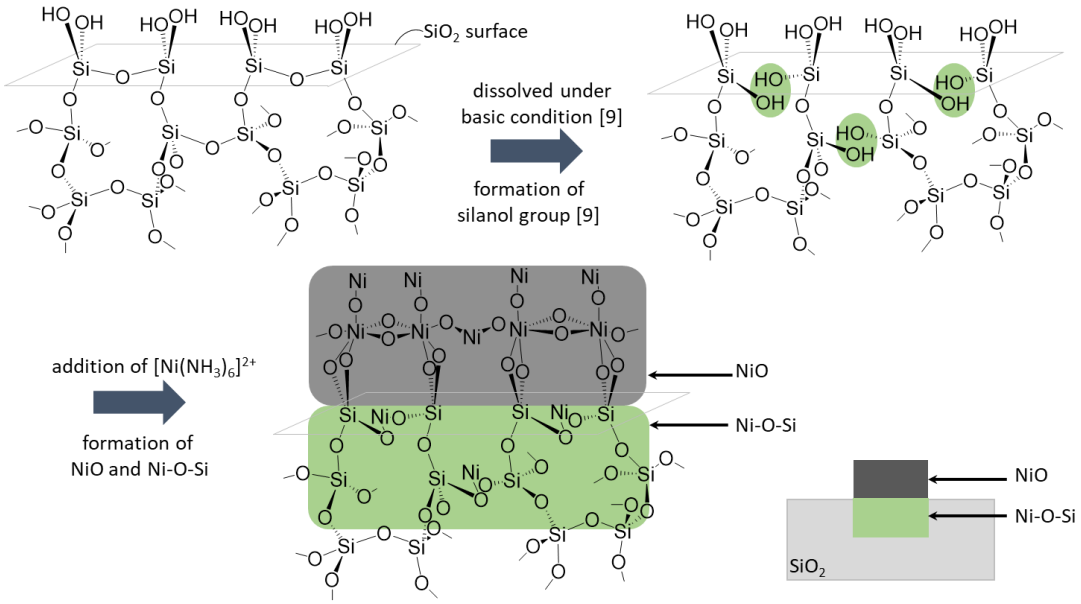

Fig. 3.4. Schematic scheme of Ni-O-Si complex structure formation.

To demonstrate the coexistence of NiO and Ni-O-Si, XANES LCF (linear combination fitting) analysis was carried out and a ratio of each component was estimated. As a consequence, XANES LCF for the NiO(amm)/SiO_2-*T* revealed the coexistence of NiO and Ni-O-Si on NiO(amm)/SiO_2-*T* and the ratio of each component was calculated as shown in Table 3.2.

Table 3.2 Pattern fitting results of NiO(amm)/SiO_2-*T*

Catalyst	Component (%)	
	NiO	Ni-O-Si
NiO(amm)/SiO_2-RT	37	63
NiO(amm)/SiO_2-573	48	52
NiO(amm)/SiO_2-773	57	43

Fitting range: 8344-8357 eV.

3.3.2. Oxidation of 1-phenylethanol

Table 3.3 and Fig. 3.5 show a result of 1-phenylethanol oxidation reaction. From the viewpoint of correlation between cluster size and catalytic activity, the smaller *CN* results in the higher yield. In fact, this size dependency was observed by the large. However, NiO(amm)/SiO_2-RT specifically showed higher activity compared to NiO(ace)/SiO_2-673 even though their *CN* was almost same.

Considering NiO(amm)/SiO_2-RT consisting of plural nickel species, namely NiO and Ni-O-Si, the coordination distance of Ni-Ni for NiO and for nickel silicate is close (0.295 nm and 0.307 nm, respectively) and these two coordination peaks were overlapped by each other. As a result, it was hard to distinguish these two coordination peak in FT, and it was difficult to discuss the NiO cluster size from *CN* only. Therefore, the cluster size of NiO(amm)/SiO_2-RT and

NiO(ace)/SiO_2-673 was estimated from TEM observation as 1.9 nm and 1.0 nm, respectively (Figs. 3.6 and 3.7). Interestingly, this result showed the larger cluster was more active than the smaller cluster, which was contrary to the size dependency. Therefore, not only cluster size but also the kind of nickel species existing on prepared catalysts was important to enhance the catalytic activity.

The result of 1-phenylethanol oxidation was reconsidered based on the kind of nickel species besides *CN*. NiO(amm)/SiO_2-RT and NiO(amm)/SiO_2-573 were more active than NiO(amm)/AC-573 and NiO(ace)/SiO_2-673 in spite of larger *CN*, which means the another factor affecting the catalysis besides the size dependency. The formation of Ni-O-Si structure with NiO nanocluster on NiO(amm)/SiO_2-*T* has been revealed by XAFS unlike the others, and it is reasonable to conclude that the interfacial Ni-O-Si structure contributed to the higher activity. In other word, the catalysts consisting of NiO and Ni-O-Si was more active compared to the others consisting of only NiO, meaning that Ni-O-Si had a promoting effect for the oxidation of 1-phenylethanol.

SiO_2 and activated carbon which were used as the support did not show the catalytic activity for the reaction, which means that NiO fixed on these support was the active species. Besides, the reaction using only nickel silicate did not proceed, therefore nickel species was not active species and it was a promoter enhancing an activity of NiO for the oxidation of 1-phenylethanol.

Table 3.3 Coordination number of Ni-Ni and yield of acetophenone[a]

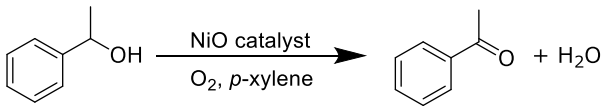

Catalyst	*CN*[b]	Yield[c] (%)	nickel species on support
NiO(amm)/SiO_2-RT	7.3±1.2	51	NiO and Ni-O-Si
NiO(amm)/SiO_2-573	7.4±1.2	28	NiO and Ni-O-Si
NiO(amm)/SiO_2-773	8.0±1.3	4.5	NiO and Ni-O-Si
NiO(amm)/AC-573	5.0±0.8	17	NiO
NiO(ace)/SiO_2-673	7.0±1.2	7.8	NiO
NiO(nit)/SiO_2-673	12.3±2.1	1.9	NiO
NiO(amm)/nickel silicate-RT	8.5±1.4	1.7	NiO
Nickel silicate	6	2.6	-
SiO_2	-	4.8	-
Activated carbon	-	2.5	-
blank	-	3.0	-

[a]1-Phenylethanol (1 mmol), NiO catalyst (0.10 g, S/C = 12), solvent: *p*-xylene (5 mL), atmosphere: O_2 (1 atm), reaction temperature: 373 K, reaction time: 6 h, [b]coordination number of the nearest Ni-Ni coordination, [c]determined by gas chromatography using an internal standard technique.

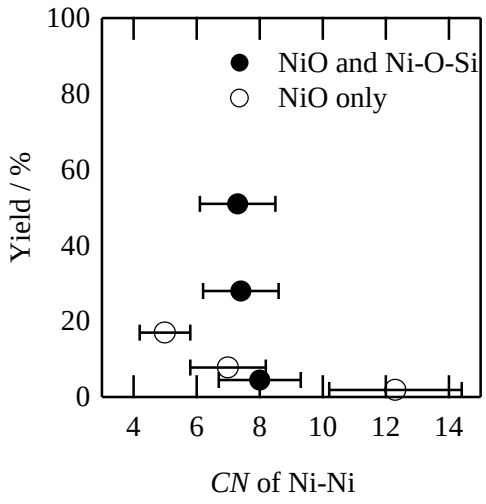

Fig. 3.5. Correlation between the yield of acetophenone and CN of the catalysts.

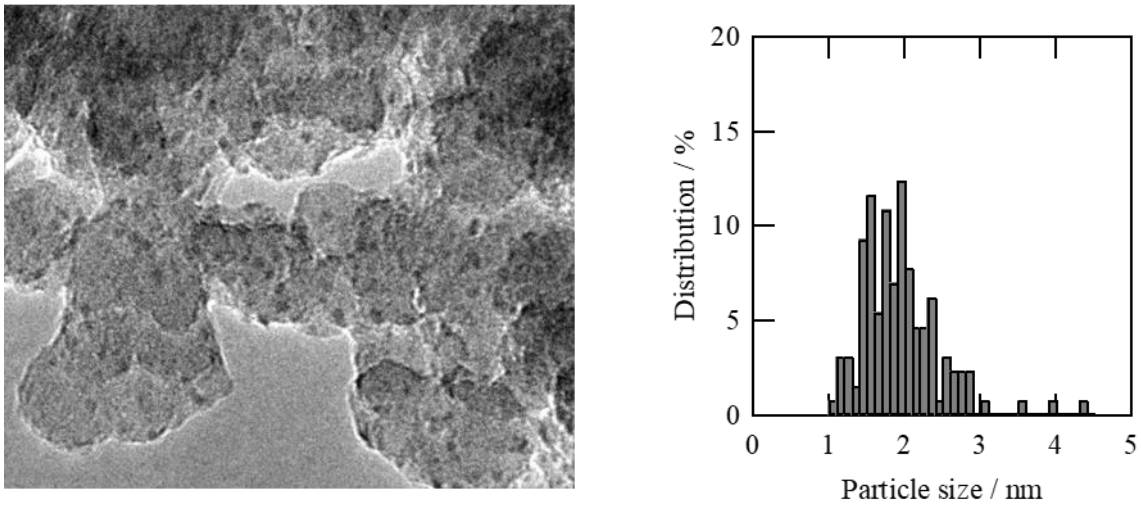

Fig. 3.6. Particle size distribution and TEM image for NiO(amm)/SiO_2-RT.

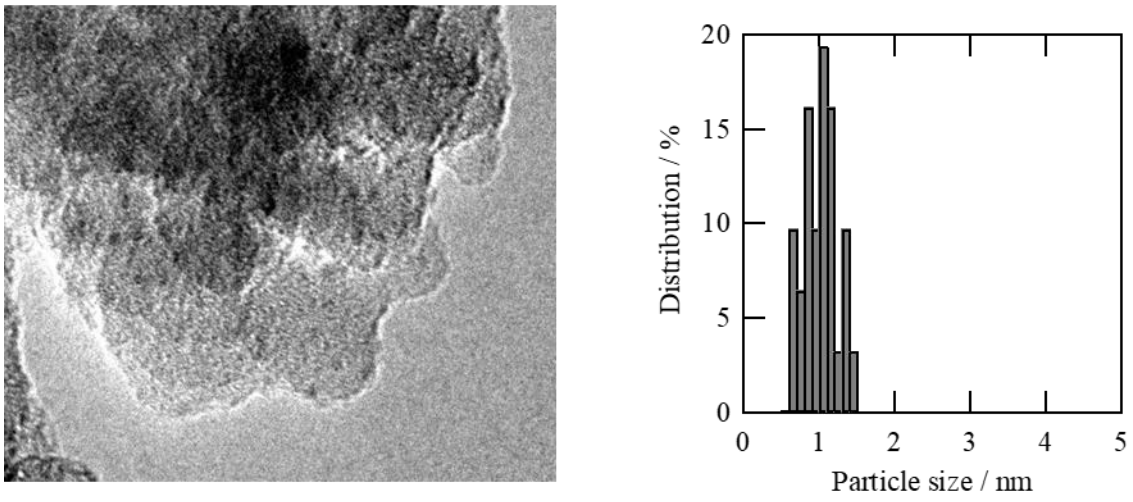

Fig. 3.7. Particle size distribution and TEM image for NiO(ace)/SiO_2-673.

Based on the result that Ni-O-Si can promote the reaction, nickel silicate supported NiO catalysts (NiO(amm)/nickel silicate-*T*) were prepared and applied to the same reaction. As a result, NiO(amm)/nickel silicate-*T* was not active contrary to an expectation that NiO(amm)/nickel silicate-*T* is also active because it possesses the Ni-O-Si structure like NiO(amm)/SiO_2-*T*. One of the considerable reasons is that NiO particle was not small sufficiently based on the *CN*. *CN* of NiO(amm)/SiO_2-773 (not active) was 8.0 and that of NiO(amm)/nickel silicate-RT was 8.5.

Moreover, XRD (Fig. 3.8) showed the aggregation of NiO as an increase of diffraction peak (Ni (200)) for NiO(amm)/nickel silicate-773 although that aggregation was not observed for NiO(amm)/SiO_2-*T*. Nickel silicate was not able to keep NiO highly disperse, resulting in the larger NiO particle than NiO(amm)/SiO_2-*T*.

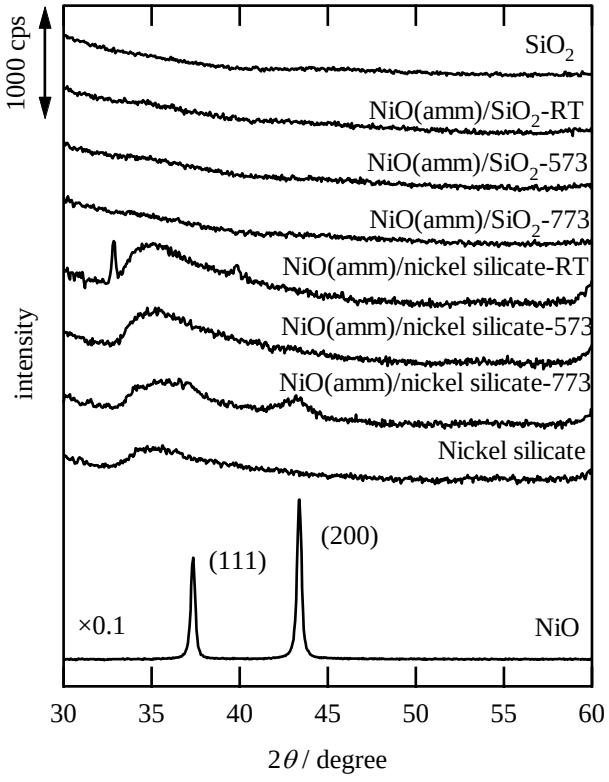

Fig. 3.8. XRD patterns of NiO(amm)/SiO_2-*T*, NiO(amm)/nickel silicate-*T* and reference compounds.

Interestingly, the activity of three NiO(amm)/SiO_2-*T* catalysts was different although their *CN* changed just slightly. Proportion of NiO and N-O-Si was estimated by XANES LCF as shown in Table 3.2 in order to reveal the reason of the drastic change of yield. XANES LCF indicated that the ration of NiO increased and that of Ni-O-Si decreased with higher temperature of calcination. Considering that Ni-O-Si existed on the interfacial region between NiO and SiO_2, that change of component ratio can be described as illustrated in Fig. 2.9. Ni-O-Si structure exposed on atmosphere transformed into NiO with the calcination, resulting in the loss of Ni-O-Si working as a promoter for the catalysis. This is the reason why the drastic diminishment of the yield was observed with the change of ratio of each nickel species, which means an importance of the interfacial region on a supported catalyst.

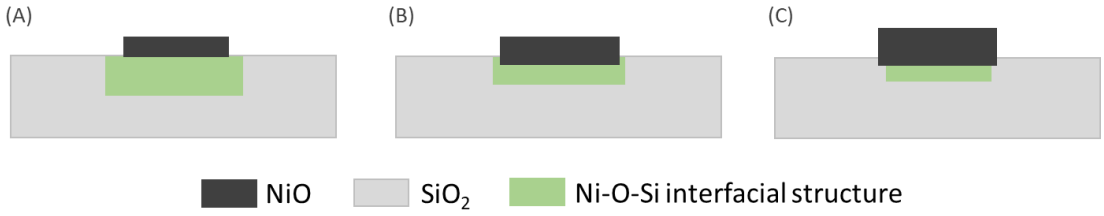

Fig. 3.9. Schematic model of NiO and the interfacial distribution on (A) NiO(amm)/SiO_2-RT, (B) NiO(amm)/SiO_2-573 and (C) NiO(amm)/SiO_2-773.

In order to know the role of the interfacial Ni-O-Si structure, CO_2 adsorption experiment was carried out for NiO(amm)/SiO_2-*T* and NiO(nit)/SiO_2-673 (Table 3.4). CO_2 adsorption on the NiO(nit)/SiO_2-673 was almost negligible. On the other hand, CO_2 adsorption on the NiO(amm)/SiO_2-*T* was noticed to some extent, indicating that a base could facilitate the dissociation of o-H bond. The amount of CO_2 adsorbed on NiO(amm)/SiO_2-*T* decreased with increasing the calcination temperature. The catalysis of the NiO(amm)/SiO_2-*T* can be explained by the amount of exposed surface of the interfacial Ni-O-Si structure having a role as a base.

Table 3.4 CO_2 adsorption on the NiO(amm)/SiO_2-*T* and NiO(nit)/SiO_2-673

Catalyst	Adsorbed CO_2 (10^{-5} mol/g_{cat})	Yield (%)
NiO(amm)/SiO_2-RT	7.2	51
NiO(amm)/SiO_2-573	2.1	28
NiO(amm)/SiO_2-773	1.6	4.5
NiO(nit)/SiO_2-673	1.5	1.9

Based on above results, Fig. 3.10 can be illustrated. Making active species smaller enable NiO catalysts to have the catalytic activity for the oxidation of 1-phenylethanol even if nickel species consisted of NiO catalyst is only NiO. However, on the other hand, the creation of Ni-O-Si structure on the interface of NiO and SiO_2 enhance the catalytic activity due to a promoting effect of Ni-O-Si structure.

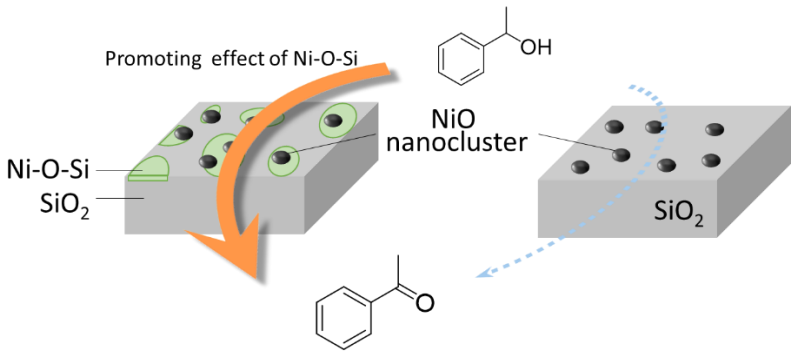

Fig. 3.10. Graphical abstract of this chapter.

3.4. Conclusion

XAFS and TEM measurements revealed that the cluster size of NiO and a kind of nickel species on prepared catalysts can be controlled by utilizing different Ni precursor, support and calcination temperature. Coexistence of NiO and Ni-O-Si structure was found on NiO(amm)/SiO_2-*T* prepared by using $[Ni(NH_3)_6](NO_3)_2$ and SiO_2 as a precursor and a support, respectively. Ni-O-Si was formed between NiO and SiO_2 as an interfacial structure, and existence of Ni-O-Si interfacial structure increased the basicity of the catalyst and promoted the dissociation of O-H bond of alcohols.

Obtained catalysts were applied for oxidation of 1-phenylethanol. As a consequence, a kind of nickel species is found to be a crucial factor for the catalysis besides particle size of active species. NiO nanocluster coexisting with Ni-O-Si was more active compared to NiO nanocluster without Ni-O-Si. Ni-O-Si can enhance the catalytic activity of NiO nanocluster as a promoter for the oxidation of 1-phenyoethanol. Creation of interfacial structure and its effective contribution is a key factor for catalyst design.

Chapter 4

Promoting the reaction by activated carbon support

4.1. Introduction

Chapter 3 mentioned the development of SiO_2 supported NiO nanocluster catalyst showing the catalytic activity to oxidation of 1-phenylethanol, and the promoting effect of interfacial Ni-O-Si structure for the reaction was found. However, in this case, two types of nickel species of NiO and Ni-O-Si produced the high catalytic activity, and it is difficult to characterize each nickel species separately. Therefore, considering active species and support separately is also important to precisely understand the catalysis of supported NiO catalyst. The precise understanding of the catalysis of the supported NiO nanocluster catalysts is expected to result in the expansion of the new catalyst design of base metal nanocluster catalysts. This is the concept of this chapter.

However, we realized the limitation of finer catalyst design by impregnation method. Using nickel ammine complex ($[Ni(NH_3)_6](NO_3)_2$) as a nickel precursor resulted in the formation of the interfacial Ni-O-Si structure besides NiO. Also, the other precursors, $Ni(NO_3)_2$ and $Ni(acac)_2$ needed a calcination at high temperature for decomposition of precursor and transformation into NiO, which indicates the difficulty of structure control. Then, colloidal method is focused on in this chapter. In this method, supported NiO catalyst is obtained by using size-controlled Ni colloid prepared in advance as a precursor [134]. By utilizing this preparation method, it is expected that finely structure-controlled NiO nanocluster can be fixed on the support without formation of the complex oxide compounds such as Ni-O-Si structure.

In the case of impregnation method, calcination is required to prepare NiO catalyst and different sized NiO catalyst is obtained because of different support. On the other hand, same sized NiO supported on different support can be obtained by using Ni colloid as a precursor since NiO is formed by oxidizing in air at room temperature, which allow understanding a function of the support in detail.

As a result, obtained catalyst was composed of only NiO nanocluster as a nickel species on the support, and a synergy effect for the catalysis between the support and the active species was found in contrast to the conventional nickel-based catalysts which were non-supported bulk catalysts. X-ray absorption fine structure (XAFS), X-ray photoelectron spectroscopy (XPS) and

in situ powder X-ray diffraction (XRD) were used to clarify the catalyst structure and the origin of catalysis.

4.2. Experimental

$NaBH_4$ was added in THF solvent and the $NaBH_4$/THF solution was refluxed in Schlenk tube for 1 h at 338 K. After synthesis of *tert*-butoxide by adding *tert*-BuOH in the $NaBH_4$/THF solution, Ni colloid was obtained by addition of dehydrated $Ni(acac)_2$ and vigorous stirring in the THF solution for 1 h at 338 K. The excess $NaBH_4$ was decomposed by the addition of *t*-BuOH.

Activated carbon (AC), Al_2O_3 or SiO_2 were dispersed into Ni colloid solution and stirred for 3 h at room temperature. After the stirring, the solvent was evaporated at 318 K in *vacuo*. Supported catalyst was washed with distilled water and dried *in vacuo* at room temperature overnight. The catalyst was denoted as NiO/AC, NiO/Al_2O_3, and NiO/SiO_2, respectively. Ni loading amount was regulated to 5 wt% for all catalysts. Process of preparing Ni colloid and fixing Ni on the support was conducted under a nitrogen atmosphere. Regarding NiO/AC, acetone and methanol were considered as a washing solvent besides water. AC supported NiO catalysts washed by acetone and methanol were denoted as NiO/AC-ace and NiO/AC-MeOH, respectively.

XAFS, XPS, and *in situ* XRD were carried out for characterization. Prepared catalysts were applied to the oxidation of 1-phenylethanol.

4.3. Results and discussion

4.3.1. Effect of support

NiO nanocluster catalysts supported on AC, Al_2O_3 and SiO_2 were prepared and applied to the liquid phase oxidation of 1-phenylethanol using molecular oxygen as an oxidant. Only AC

supported NiO catalyst showed catalytic activity for the reaction (Table 4.1), and AC was regarded as an appropriate support for this catalytic system and used for the reaction below. This result means AC is an appropriate support for this catalytic system. Interesting thing is that only NiO/AC was active for the reaction although a NiO particle size of all catalysts might be same since the particle size was regulated during the preparation of Ni colloidal solution which is precursor. In other word, there is another factor affecting the catalysis besides NiO particle size and AC assisted something for the reaction.

Table 4.1 Acetophenone yield of 1-phenylethanol oxidation reaction

Catalyst	Yield (%)
NiO/AC-ace	83
NiO/AC-MeOH	65
NiO/AC	36
NiO/SiO_2	3.2
NiO/Al_2O_3	2.7
AC	4.4
blank	3.1

1-Phenylethanol (1 mmol), NiO catalyst (0.10 g, S/C ratio = 12), solvent: *p*-xylene (5 mL), temperature: 423 K, reaction time: 24 h, atmosphere: air (1 atm). S/C ratio is mol ratio of substrate to $catalyst_{Ni}$.

Ni *K*-edge XANES (X-ray absorption near edge structure) of NiO/AC, NiO/Al_2O_3, and NiO/SiO_2 were similar not to Ni foil but to bulk NiO in terms of shape and edge position as shown in Fig. 4.1, indicating that three of the catalysts were successfully oxidized at room temperature in air. It can be said that valence and chemical species were the same among these catalysts regarding XANES shape. In other word, a unique nickel species besides NiO did not exist on NiO/AC to be active for the reaction. Hence, the difference of activity was not explained by XANES analysis.

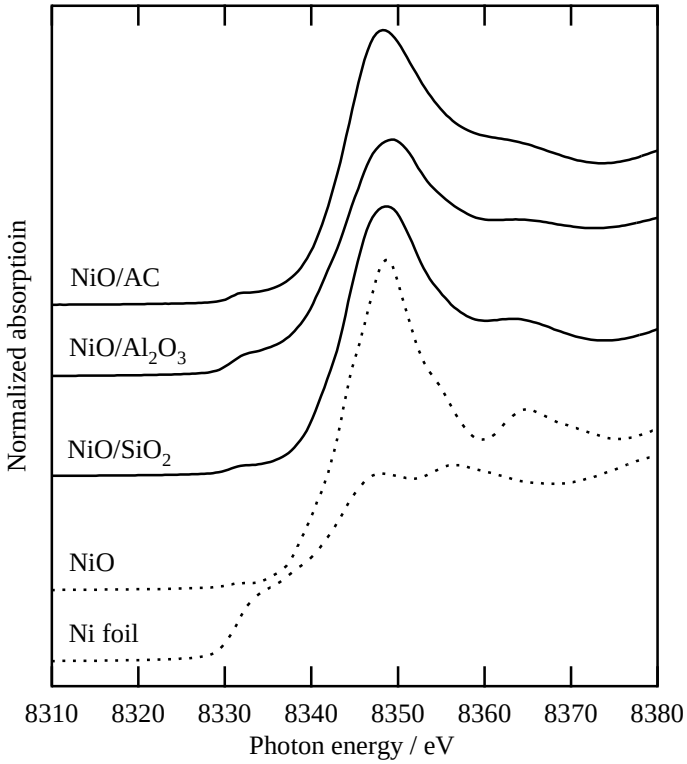

Fig. 4.1. Ni *K*-edge XANES of NiO catalysts (solid line) and reference compounds (dotted line).

In order to demonstrate whether NiO fixed on prepared catalysts is nanocluster, the analysis of EXAFS (Extended X-ray absorption fine structure) region was conducted. Fig. 4.2 shows a Fourier transformation of the EXAFS function of NiO/AC, NiO/Al_2O_3 and NiO/SiO_2. Peaks at around 0.29 nm corresponds to Ni-(O)-Ni coordination of the oxidized nickel species, and its intensity gives information about cluster size. In general, it can be said that the smaller clusters result in the smaller intensity since the smaller clusters have the larger surface area. The Peak intensity of all catalysts was weaker than the reference compound, which means that NiO of prepared catalysts was nanocluster.

The result of *in situ* XRD analysis is shown in Fig. 4.3. *In situ* XRD of NiO/AC, NiO/Al_2O_3 and NiO/SiO_2 consisted in heating from 473 K to 723 K under a H_2/He mixed gas flow and collecting patterns along the thermal treatment. To remove the background influence, all diffractograms were subtracted by a signal of the machine. Ni metal was observed with rising temperature, but no peak of NiO at RT was observed on all catalysts, which indicates that NiO fixed on the supports was nanocluster, which corresponds to the discussion of EXAFS (FT).

Based on the above results, the facts that NiO nanocluster is fixed on the support is same among different supported NiO catalyst. Therefore, the role of AC is a key factor for the catalysis besides the cluster size and kinds of nickel species.

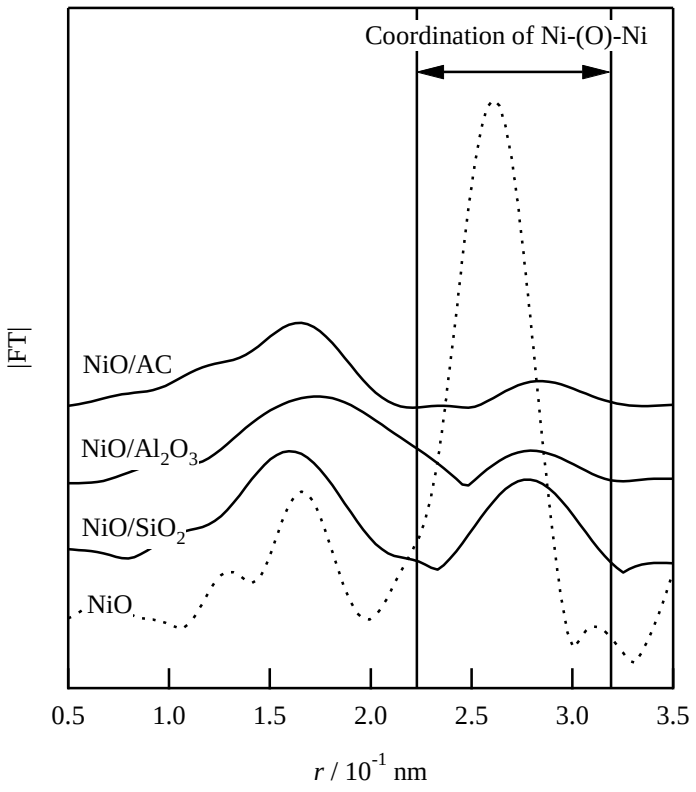

Fig. 4.2. FT of Ni *K*-edge EXAFS for NiO catalyst.

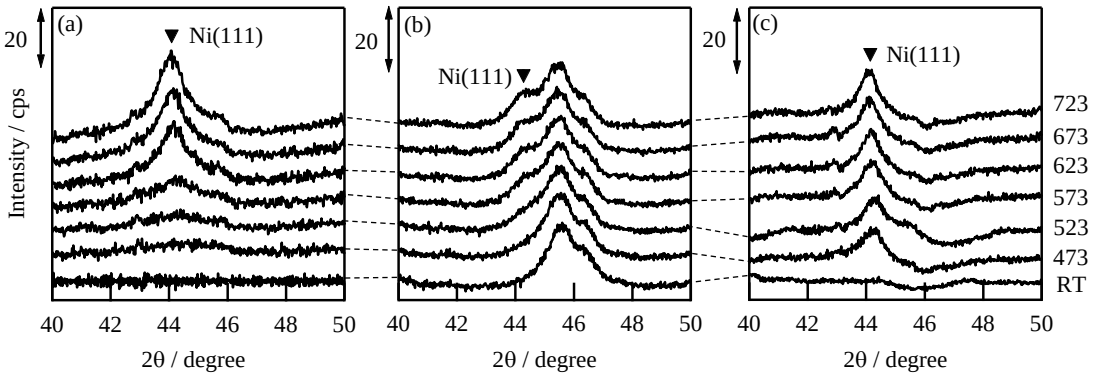

Fig. 4.3. *in situ* XRD patterns of (a) NiO/AC, (b) NiO/Al_2O_3 and (c) NiO/SiO_2-ace. The catalysts were heated from 473 K to 723 K under a H_2/He mixed gas flow.

To obtain the information about a role of AC, XPS measurement was carried out for NiO/AC, NiO/Al_2O_3 and NiO/SiO_2 as shown in Fig. 4.4. The spectra of nickel species exhibit the main peak around 856 eV that is attributed to Ni $2p_{3/2}$ (+2) [143]. Herein, no peak shift was observed, suggesting that there is no difference of electronic state among these catalysts.

Based on the above results, chemical state, cluster size and electronic state of nickel species of these catalysts are same. In other word, AC affected not NiO but reactants, which means that AC directly contributed to the appearance of the catalysis by interacting with the reactant. Discussion of the AC's role is mentioned in section 4.3.3, section of reaction mechanism, in detail.

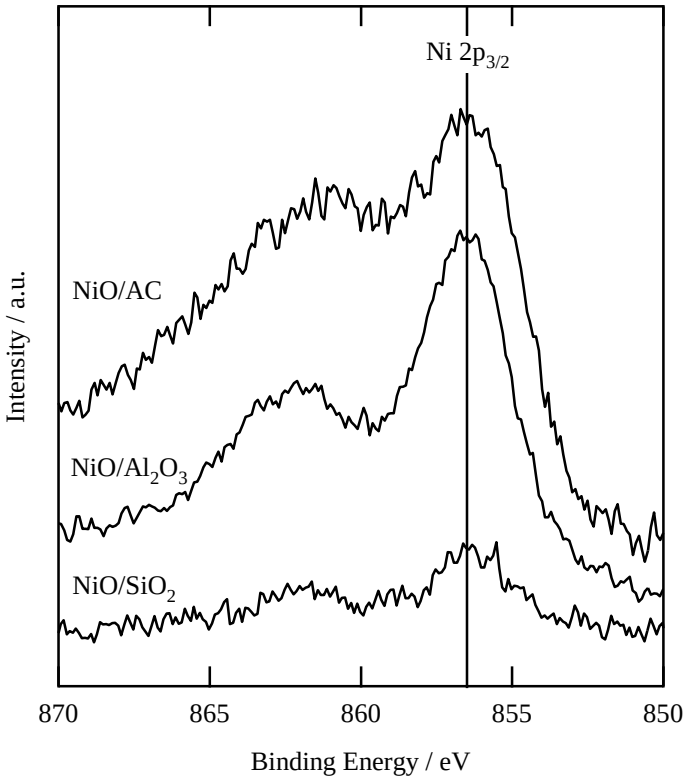

Fig. 4.4. XPS of Ni $2p_{3/2}$ for NiO catalysts.

4.3.2. Effect of solvent during the washing step

Before discussing the role of AC and reaction mechanism in detail, the effect of solvent used for the catalyst washing step is mentioned in this section.

NiO catalysts were prepared by using Ni colloid as a precursor in this work. Ni clusters dispersing in the Ni colloid was regulated in nano scale, and its surface was highly active against external environment. Therefore, it is possible to obtain NiO by oxidizing even at room temperature in the air. On the other hand, washing of catalysts was carried out after fixing Ni colloid on the support, namely while the nickel species is oxidized, therefore the solvent used for washing step can affect the chemical state of nickel species.

AC supported NiO catalysts washed with acetone or methanol were prepared (they are denoted as NiO/AC-ace and NiO/AC-MeOH, respectively) besides NiO/AC (washed by water). These catalysts were applied for the 1-phenylethanol oxidation and characterized by XAFS to reveal the effect of solvent during washing step.

Table 4.1 shows also results of 1-phenylethanol oxidation using NiO/AC washed with different solvents, and as a result, different solvents led to different yields of acetophenone. XAFS measurements were carried out to reveal a reason why the solvents used for washing process affected the catalytic activity from the viewpoint of chemical state.

Fig. 4.5 shows Ni *K*-edge XANES of NiO/AC catalysts and reference compounds. Based on the XANES shape, three of NiO/AC catalysts consist of not metallic Ni but oxidized Ni. However, no difference of chemical state was observed among three of NiO/AC catalysts and XANES could not reveal the reason why the catalytic activity was affected by solvents using for washing step. Therefore, the analysis of EXAFS region was carried out to obtain the information about chemical state of the catalysts in detail.

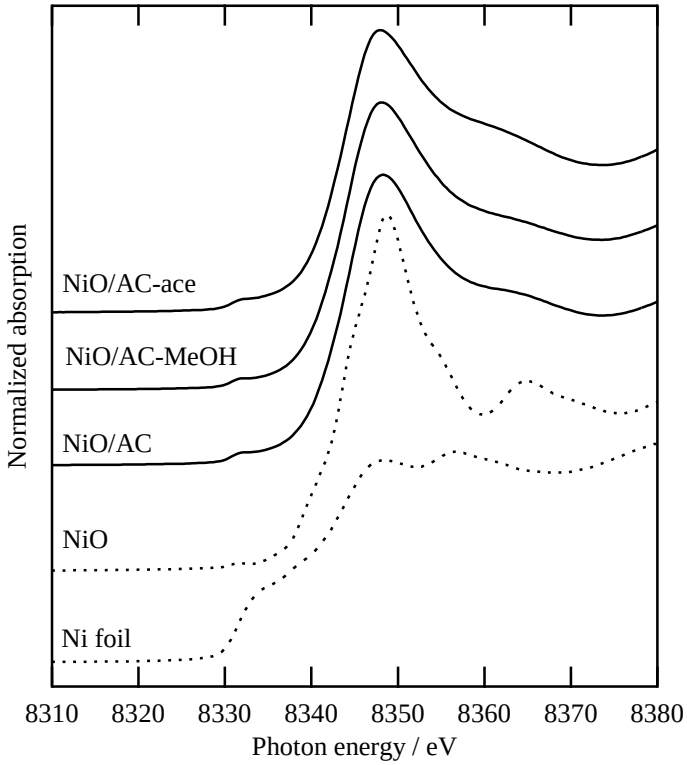

Fig. 4.5. Ni *K*-edge XANES of NiO catalysts (solid line) and reference compounds (dotted line).

In order to reveal the difference of chemical species causing the change of catalytic activity among three of NiO/AC catalysts washed with different solvents, the analysis of EXAFS region was carried out.

Fig. 4.5 and Table 4.2 are FT of EXAFS function for NiO/AC catalysts and results of curve fitting analysis for the nearest Ni-(O)-Ni coordination, respectively. The analysis of EXAFS showed the different coordination distance of Ni-(O)-Ni coordination (*r*) as shown in Fig. 4.5 and Table 4.2. Herein, the *r* of NiO/AC-ace, NiO/AC-MeOH, NiO/AC, NiO, and $Ni(OH)_2$ is 0.299, 0.308, 0.313, 0.295, and 0.313 nm, respectively. The *r* changed between 0.295 nm and 0.313 nm, namely between NiO and $Ni(OH)_2$. This result seemed to mean that NiO and $Ni(OH)_2$ exist on three of NiO/AC catalysts, and the ratio of each nickel species was varied by different solvents. In other word, the *r* corresponds to the ratio of NiO and $Ni(OH)_2$, and the order of NiO ratio is NiO/AC-ace > NiO/AC-MeOH > NiO/AC. The order of the yield (Table 4.1) corresponded to the ratio of NiO, which indicates that NiO is the active species for the reaction and the more NiO ratio resulted in the higher yield. It was found that NiO is the active species for the reaction and it is important to choose an appropriate solvent for catalyst washing process.

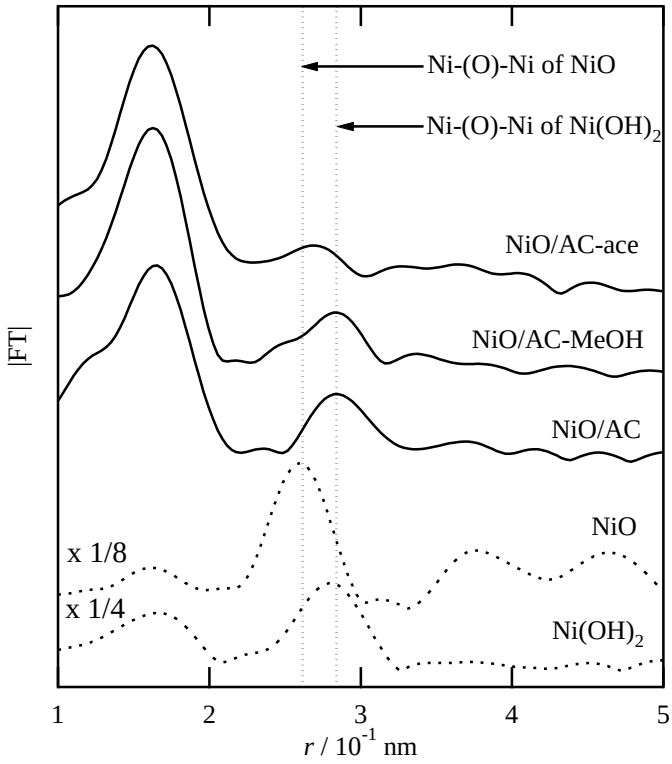

Fig. 4.6. FT of Ni *K*-edge EXAFS for NiO catalysts (solid line) and reference compounds (dotted line).

Table 4.2 Curve fitting results of the nearest Ni-Ni coordination for NiO catalysts and reference compounds

Catalyst	FR[a] (nm)	CN[b]	r[c] (nm)	dE[d] (eV)	DW[e] (nm)
NiO/AC-ace	0.233-0.295	3.6±0.5	0.299±0.001	3.87±1.16	0.0145±0.0013
NiO/AC-MeOH	0.264-0.312	3.4±1.6	0.308±0.001	7.27±1.05	0.0128±0.0012
NiO/AC	0.255-0.331	2.9±0.5	0.313±0.001	9.00±1.21	0.0119±0.0014
NiO (model)	0.224-0.298	12	0.295	0.00	0.0060
$Ni(OH)_2$ (model)	0.239-0.322	6	0.313	0.00	0.0060

[a]Filtering range, [b]coordination number of Ni-(O)-Ni, [c]coordination distance, [d]difference between the model compound and experimental threshold energies, [e]Debye-Waller factor. FT range: 30-130 nm^{-1}.

4.3.3. Reaction mechanism

The reaction mechanism including the role of NiO and AC is discussed in this section. First of all, an experiment was conducted as follows to reveal the role of NiO which is the active species.

In order to obtain information about a role of NiO, NiO catalysts with and without 1-phenylethanol were prepared for XAFS measurements (denoted as NiO/AC-ace-PhEt and NiO/AC-ace, respectively). NiO/AC-ace-PhEt: A few drops of 1-phenylethanol were dropped onto a pellet of the NiO catalyst prepared for the XAFS measurement. Then this pellet was analyzed. NiO/AC-ace: It was a just as-prepared NiO catalyst. Fig. 4.3 is FT of NiO/AC-ace-PhEt, NiO/AC-ace, and NiO. Curve fitting analysis of FT for Ni-O coordination was conducted as shown in Table 4.3, CN of NiO/AC-ace-PhEt was greater than that of NiO/AC-ace. The increase of CN for Ni-O coordination means the adsorption of OH group of 1-phenylethanol on NiO. In other word, Ni atom of NiO interacted with O atom of 1-phenylethanol, and the adsorption of 1-phenylethanol on NiO was one of the elementary reactions as shown in Fig. 4.7.

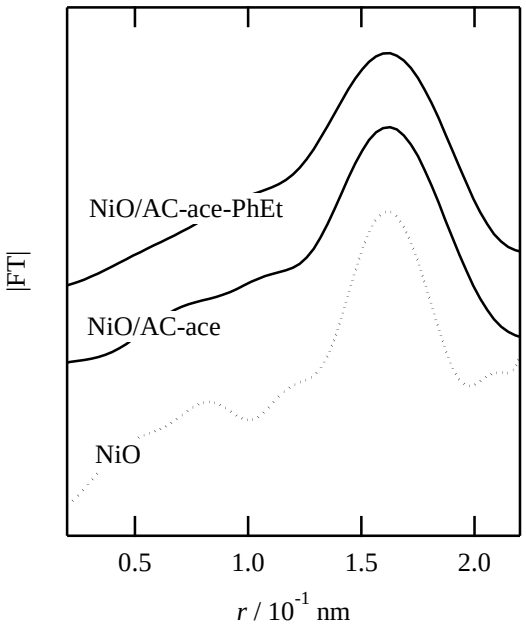

Fig. 4.6. FT of Ni *K*-edge EXAFS for 1-phenylethanol adsorbed NiO catalyst (NiO/AC-ace-PhEt), as-prepared NiO catalyst (NiO/AC-ace), and NiO.

Table 4.3 Curve fitting results of Ni-O coordination for as-prepared NiO catalysts and 1-phenylethanol adsorbed NiO catalyst

Catalyst	CN[a]	r^b(nm)	dE^c (eV)	DW[d] (nm)
NiO/AC-ace-PhEt	8.7±1.3	0.206±0.0011	3.51±2.08	0.0096±0.0016
NiO/AC-ace	7.4±1.1	0.206±0.0011	3.91±2.04	0.0087±0.0016
NiO (model)	6	0.209	0.00	0.0060

[a]Coordination number, [b]coordination distance, [c]difference between a model compound and experimental threshold energies, [d]Debye-Waller factor. Filtering range: 0.135-0.193 nm, FT range: 30-130 nm^{-1}.

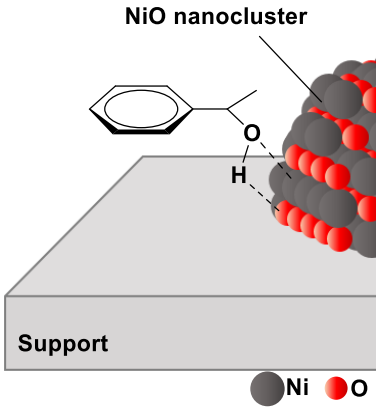

Fig. 4.7. Adsorption of 1-phenylethanol on NiO.

A report mentioning Nano-sized NiO's Lewis acidity of Ni^{2+} [102] also corresponds to the adsorption of 1-phenylethanol described in Fig. 4.7. In addition, Ni^{2+} of Nano-sized NiO has an ability to subtract α-hydride (α-C-H) in contrast to bulk NiO [103]. Therefore, a reaction mechanism of 1-phenylethanol oxidation using NiO catalyst without an assist of the support can be illustrated as shown in Fig. 4.8. Adsorption of 1-phenylethanol on NiO weakens a bond of O-H, O and Ni of NiO dissociated O-H bond and subtract α-hydride, respectively, resulting in the production of acetophenone.

Herein, there are three key steps in the reaction: step i) dissociation of hydroxyl O-H bond, step step ii) extraction of α-hydride (α-C-H), and iii) subtraction of H (O-H). The

adsorption of OH group on NiO site mentioned above promotes the step i). Therefore, assist of step ii) and iii) is expected to lead to the higher activity. An idea here is that AC can promote step ii) or iii), and this is the reason why only AC supported NiO catalyst is active for the reaction.

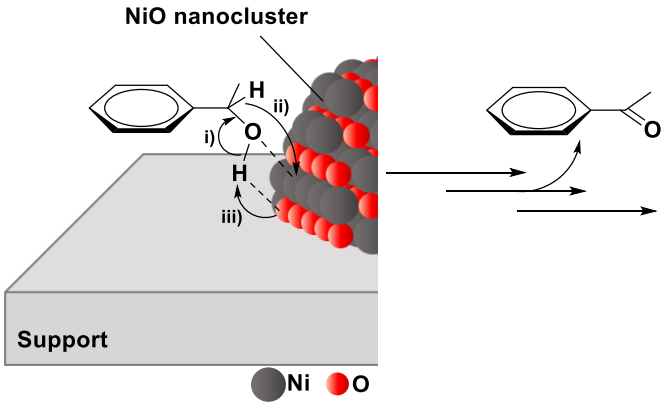

Fig. 4.8. A part of reaction mechanism for the oxidation of 1-phenylethanol using NiO catalyst.

The adding hydroquinone as a radical scavenger decreased the reaction rate drastically as shown in Table 4.4, indicating the production of a radical intermediate in the reaction process. It is reasonable to say that AC generated the radical intermediate, based on the results that only NiO/AC catalysts showed the activity although no difference of chemical and electronic state among NiO/AC, NiO/Al_2O_3, and NiO/SiO_2. Moreover, the radical intermediate seemed to be produced by subtracting α-H (α-C-H) since the dissociation energy of αC-H bond is much lower (84 kcal·mol^{-1}) compared to that of O-H bond (103 kcal·mol^{-1}) [144, 145]. Therefore, AC promoted the step ii) in Fig. 4.8, resulting in the catalytic activity on NiO/AC.

Table 4.4 Acetophenone yield of 1-phenylethanol oxidation reaction[a]

Catalyst	Yield (%)
as-prepared NiO/AC-ace	39
NiO/AC-ace + Hydroquinone[b]	1.7

[a]1-Phenylethanol (1 mmol), NiO catalyst (0.10 g, S/C ratio = 12), solvent: *p*-xylene (5 mL), reaction time: 3 h, atmosphere: air (1 atm). [b]Hydroquinone: 0.25 mmol. [c]treated in *vacuo* at 723 K for 1 h. S/C ratio is mol ratio of substrate to $catalyst_{Ni}$.

The reaction rate decreased with time, and the reaction stopped after approximately 14 h due to the equilibrium (Table 4.5, Fig. 4.9), and the reaction was a first-order reaction since a linear relation between ln*C* and time (Fig. 4.10). *C* is the concentration of 1-phenylethanol in the Schlenk tube during the reaction. In addition, the same amount of hydrogen was observed as production of acetophenone, which means that hydrogen molecule is produced as a byproduct. The production of hydrogen was observed by measuring the change of pressure of gas generating during the reaction in glass line.

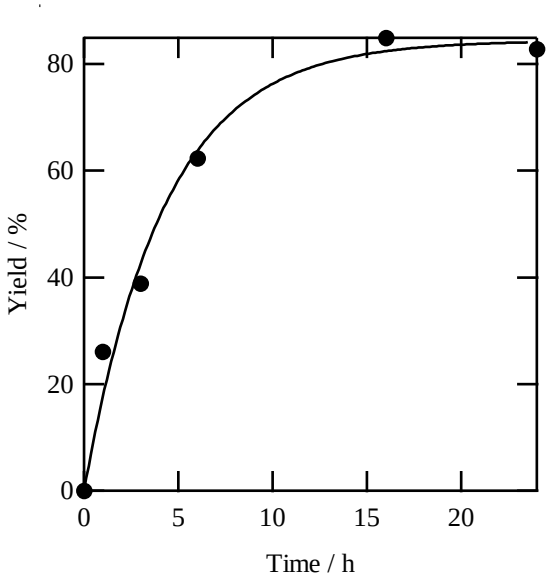

Fig. 4.9. Time profile of yield for oxidation of 1-phenylethanol on NiO/AC-ace.

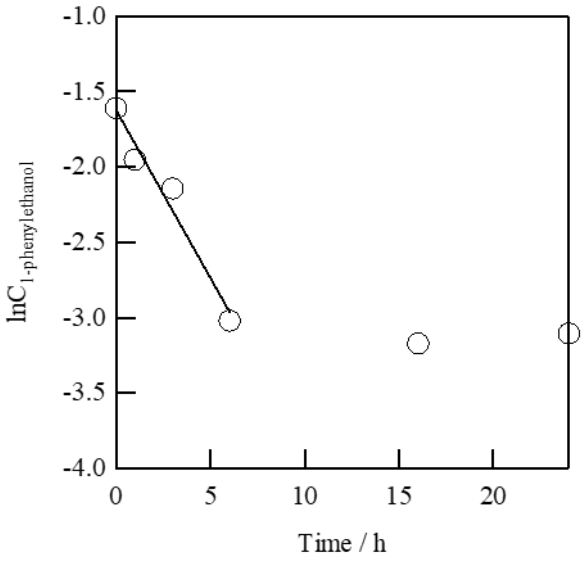

Fig. 4.10. ln*C* versus time for oxidation of 1-phenylethanol by NiO/AC-ace; *C* is the concentration of 1-phenylethanol.

Table 4.5 Time profile of yield for 1-phenylethanol oxidation.

Time (h)	Yield (%)
1	26
3	39
6	62
16	85
24	83

1-Phenylethanol (1 mmol), NiO catalyst (0.10 g, S/C ratio = 12), *p*-xylene (5 mL), temperature (423 K), atmosphere: air (1 atm). S/C ratio is mol ratio of substrate to catalyst$_{Ni}$.

As a consequence, proposed reaction mechanism can be drawn as shown in Fig. 4.11. At first, 1-phenylethanol adsorbs on NiO nanocluster (path i), leading to the beginning of the reaction. Secondary, AC subtracts α-hydrogen and the radical intermediate is produced (path ii). O-H bond is dissociated by NiO nanocluster and acetophenone is produced (path iii). Finally, hydrogen molecule is produced and the active site is regenerated (path iv). The same amount of gas generation as acetophenone production was observed experimentally.

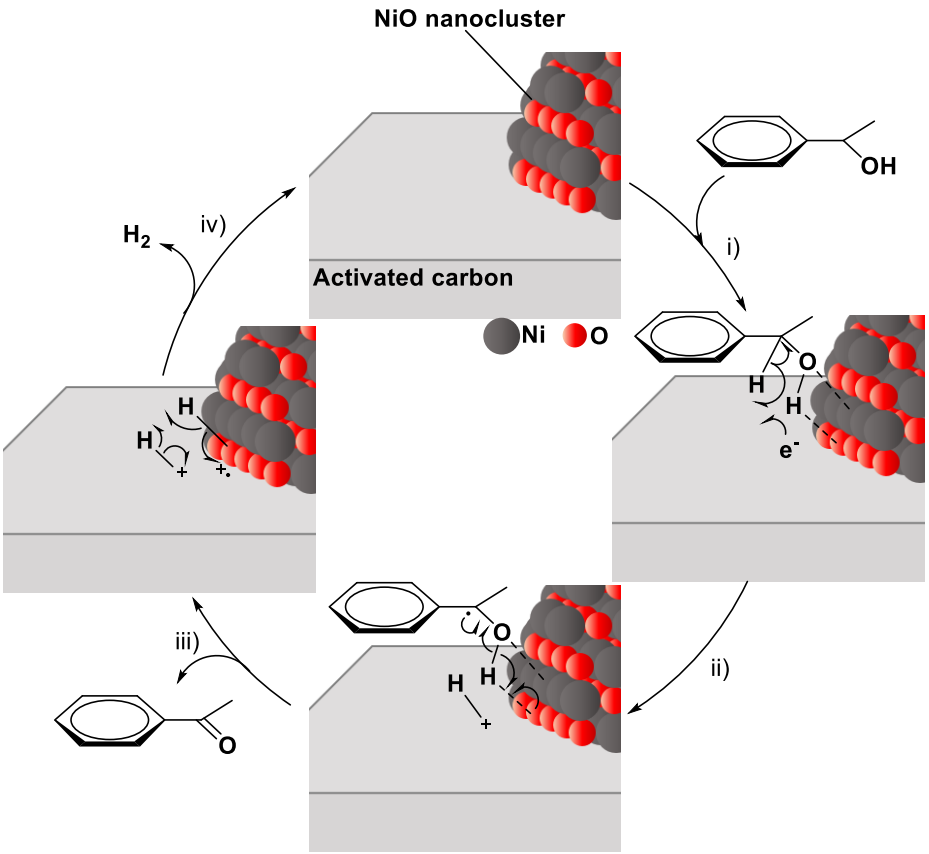

Fig. 4.11. The plausible mechanism of oxidation of 1-phenylethanol with NiO catalysts; i) adsorption of 1-phenylethanol on NiO nanocluster, ii) subtraction of α-hydride by AC, iii) production of acetophenone, iv) production of hydrogen and regeneration of the catalyst.

As mentioned above, the existence of hydroquinone disturbed the reaction drastically. Therefore, path v-vii in Fig. 4.12 can be described. As shown in Fig. 4.12 (path v-vii), the hydroquinone led to the consumption of the radical intermediate and to the former state of the catalytic cycle.

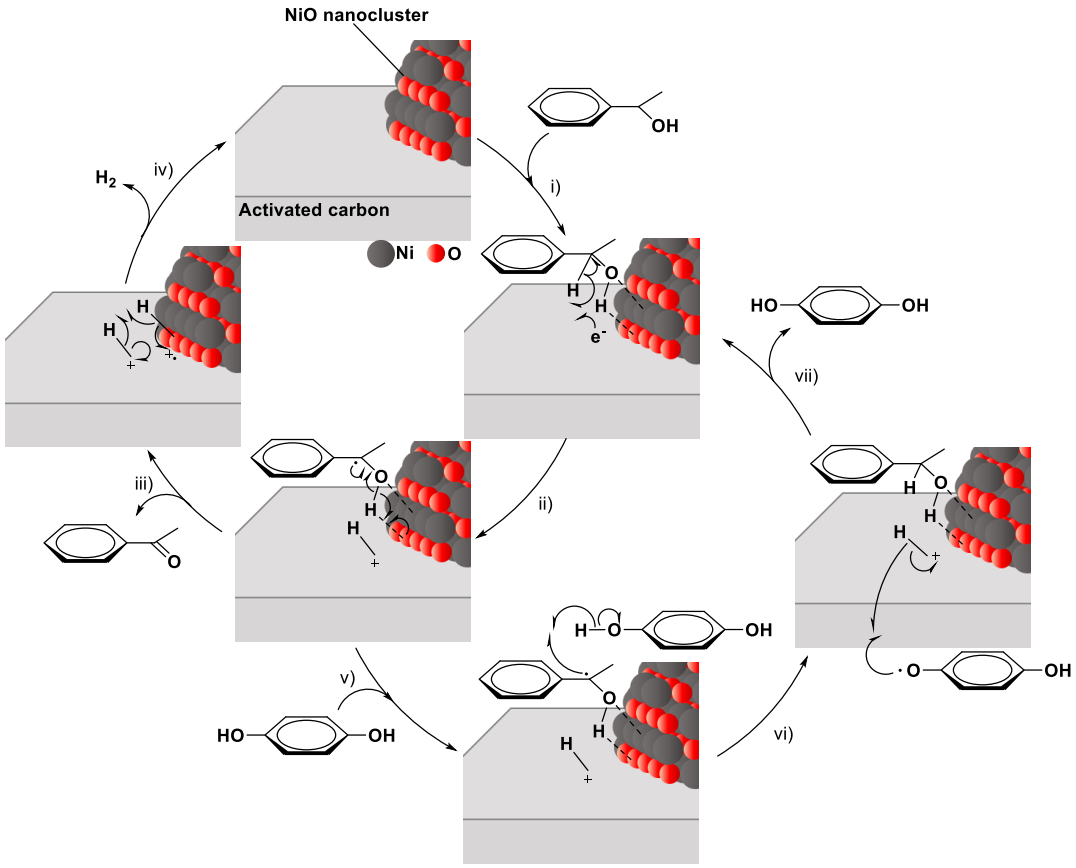

Fig. 4.12. The plausible mechanism of oxidation of 1-phenylethanol with NiO catalysts.

4.4. Conclusion

Supported NiO nanocluster catalysts were prepared by using Ni colloid as a precursor. Obtained catalysts had the activity for liquid phase oxidation of -1phenylsthanol using molecular oxygen under base-free condition.

NiO nanocluster was fixed on different supports (AC, SiO_2, and Al_2O_3), and only AC supported NiO nanocluster showed the activity for the reaction. Based on the results that no difference of chemical and electronic state among three of supported NiO catalysts, and that the reaction proceeded as a radical reaction, it can be said that AC's ability to produce a radical intermediate generated the catalytic activity of NiO/AC catalysts for the reaction.

The ratio of NiO and $Ni(OH)_2$ was controlled by using different solvent for the catalyst washing step. NiO/AC-ace consisting of the greatest NiO population showed the highest activity among three of NiO/AC catalysts, which indicates that the active species for the reaction was NiO and that more NiO ratio facilitated the adsorption of 1-phenylethanol to the catalyst, leading to more yield of acetophenone.

This work not only developed the new NiO catalyst for the oxidation of 1-phenylethanol but also obtained the insight of the reaction mechanism via X-ray analyses.

Chapter 5

Promoting the reaction by hydrotalcite support

5.1. Introduction

In chapter 4, the subtraction of α-hydride (step ii of Fig. 4.8) was promoted by activated carbon. On the other hand, in chapter 5, promoting the dissociation of O-H bond (step iii of Fig. 4.8) was focused on to enhance the catalytic activity. Metal oxides and clay minerals such as Al_2O_3, MgO and hydrotalcite can dissociate O-H bond by subtracting H^+ as a Brønsted base, hydrotalcite was utilized as a support in this chapter.

Since Ni-incorporated hydrotalcite showed catalytic activity for the oxidation of alcohols [74, 75], the synergic combination of nickel and hydrotalcite is expected to be effective for the reaction. Dispersing NiO nanocluster on hydrotalcite is expected to be more favorable for the reaction. The supported NiO catalysts were prepared by using Ni colloid as a precursor and applied for the oxidation of benzyl alcohol and 1-phenylethanol. I attempted to develop a higher active supported NiO nanocluster catalyst, to clarify the reaction mechanism, and to find out the role of support and interfacial structure.

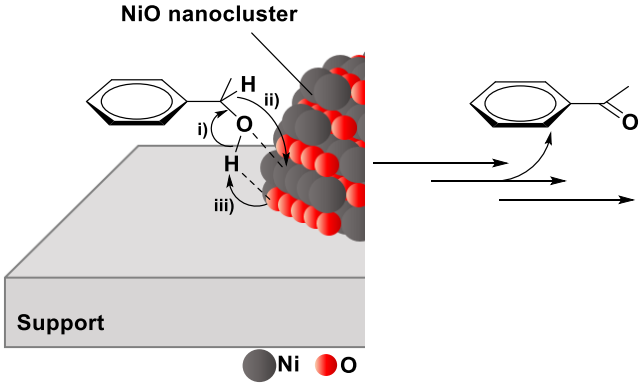

Fig. 4.8. A part of reaction mechanism for the oxidation of 1-phenylethanol using NiO catalyst.

5.2. Experimental

Preparation of Ni colloid was conducted in an ice bath under a nitrogen atmosphere. PVP and $Ni(NO_3)_2 \cdot 6H_2O$ (PVP/Ni = 6) were dissolved by water (20 mL) in a Schlenk tube. $NaBH_4$ aq was injected in the Schlenk tube, resulting in the production of nickel colloid. Hydrotalcite (HT) was dispersed into Ni colloid solution, followed by stirring for 1 h. After the stirring, the catalyst was washed with distilled water and dried *in vacuo* at room temperature overnight. Ni loading amount was regulated to 5 wt%. Prepared catalyst was denoted as NiO/HT. XAFS was carried out for characterization. Prepared catalysts were applied to the oxidative dehydrogenation of 1-phenylethanol and benzyl alcohol.

5.3. Results and Discussion

5.3.1. XAFS measurement

XANES profile of prepared catalyst was collected in order to find out the chemical state of nickel species supported on HT. Fig. 5.1 shows the XANES spectra of prepared catalyst and reference compounds. Based on the XANES shape, prepared catalyst was similar not to Ni foil but to NiO, which means that nickel species supported on HT was the oxidized nickel species like NiO. However, regarding the energy position of white line, the position of the prepared catalyst was higher than NiO. This result indicates that another nickel species which is not NiO was contained in the prepared catalyst. Clarifying the component consisting of NiO/HT is one of the most important thing in order to make the correlation of catalyst structure and activity clear. I tried to find another nickel species to make paper better.

HT used in this work can be illustrated as Fig. 5.2 [146]. Hydrotalcite is a clay mineral containing Al and Mg in its framework. Ni-O-M (M = Al or Mg) bond is formed on the interface between NiO and HT when NiO was supported on HT (Fig. 5.2). This interfacial structure (Ni-

O-M) can be regarded as another nickel species, and the XANES profile seemed to reflect the interfacial structure.

Hence, Ni-incorporated hydrotalcite (inc-Ni-HT) was prepared as a bulk compound of the Ni-O-M structure by reported method [74], and its XANES was collected (Fig. 5.1). As shown in Fig. 5.1, the energy position of inc-Ni-HT is higher than NiO, and that of NiO/HT is between NiO and in-Ni-HT, which proves the formation of Ni-O-M as a nickel species of NiO/HT besides NiO.

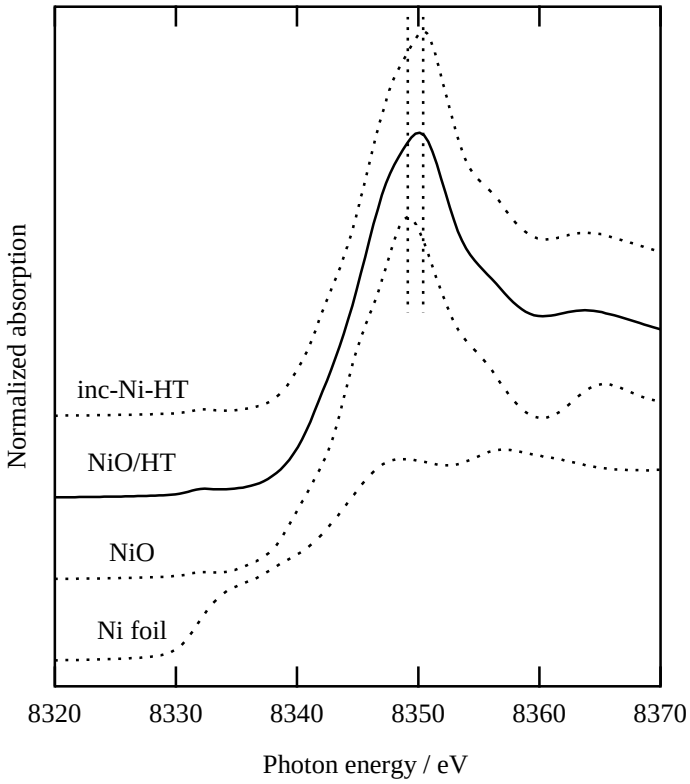

Fig. 5.1. Ni *K*-edge XANES of NiO/HT and reference compounds.

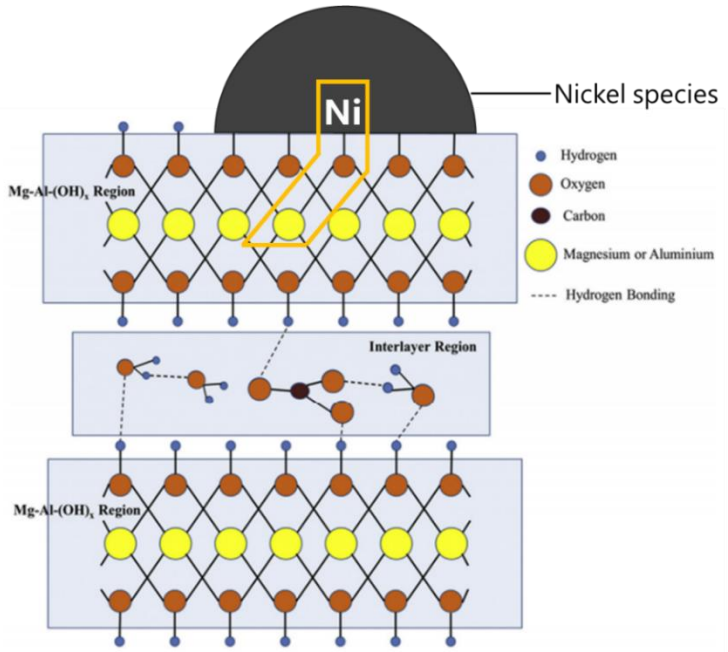

Fig. 5.2. Schematic structure of the prepared catalyst supported on hydrotalcite [146].

Linear combination fitting (LCF) of XANES was carried out using NiO and inc-Ni-HT as a reference compound, in order to prove the coexistence of NiO and Ni-O-M, and to estimate the ratio of each component. The calculated spectrum fitted the observed spectrum finely as shown in Fig. 5.3, and the ratio of each component was estimated as shown in Table 5.1. LCF revealed the coexistence of NiO and Ni-O-M as a result. The large ratio of inc-Ni-HT (Ni-O-M) seemed to be caused by NiO nanocluster possessing large surface area of interface between NiO and HT. In other word, NiO nanocluster is successfully supported on HT.

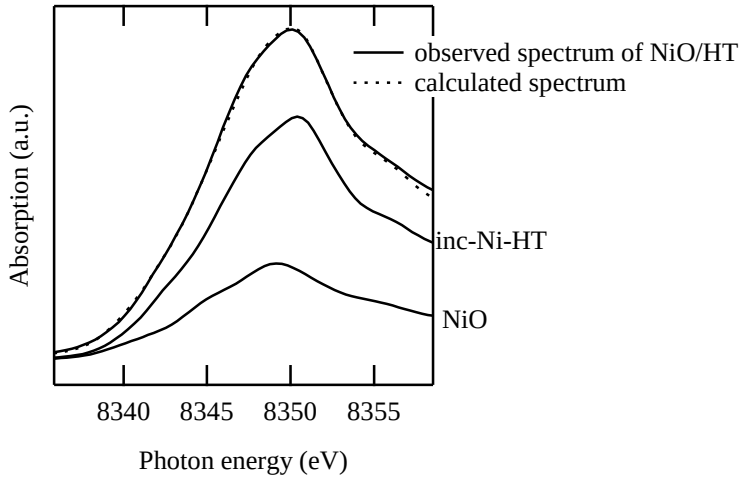

Fig. 5.3. Linear combination fitting analysis

Table 5.1 Result of linear combination fitting analysis

Component	Ratio (%)
inc-Ni-HT (Ni-O-M)	70
NiO	30

Fitting range: 8336-8358 eV.

5.3.2. Oxidation of benzyl alcohol and 1-phenylethanol

The comparison between the catalysts prepared in this chapter and conventional nickel-based catalysts for oxidation of benzyl alcohol is shown in Table 5.2. Regarding three of the reported catalysts (ref.:75-77), excess amount of catalyst to substrate was used for the reaction (S/C ratio is less than 1.0), which means that these catalysts did not work ideally as a catalyst. On the other hand, in the case of the catalyst reported in ref. 74, a catalyst amount of inc-Ni-HT was used for the reaction (S/C ratio=3.1) and the yield of benzaldehyde was 27 mmol/g_{catNi}. Herein, comparing with ref 74, NiO/HT prepared in this work was two times more active although reaction atmosphere is milder (this work: O_2 1 atm balloon, reference 74: O_2 bubbling of 6 mL/min). Dispersing NiO nanocluster on hydrotalcite led to the higher activity compared to the

Ni incorporated hydrotalcite which is a bulk compound. It can be said that the most active nickel-based catalyst for the oxidation dehydrogenation of benzyl alcohol was developed in this work.

Table 5.2 Comparison of activity between Ni-HT and conventional nickel-based catalysts[a]

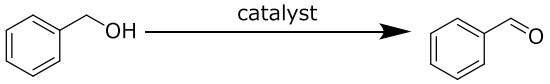

Catalyst	Atm.	Temp. (K)	Time (h)	Yield (mmol/g_{catNi})	S/C ratio	Ref.
NiO/HT[b]	O_2 (1 atm)	333	6	52	12	this work
inc-Ni-HT	O_2 (6 mL/min)	333	6	27	3.1	74
inc-Ni-HT	O_2 (10 mL/min)	353	8	7.5	0.45	75
NiO_2	O_2 (1 atm)	363	6	5.1	0.30	77
$Ni(OH)_2$	O_2 (1 atm)	363	1	5.2	0.31	76

[a] See the reference for the detailed information of the catalysts. [b] Benzyl alcohol: 1 mmol, catalyst: S/C ratio = 12, toluene: 5 mL. S/C ratio is mol ratio of substrate to $catalyst_{Ni}$.

The catalytic activity for the oxidation of 1-phenylethanol using prepared catalysts in this work was compared in Table 5.3. The yields of acetophenone at same reaction time (6 h) were determined via gas chromatography using internal standard method. NiO/SiO_2-RT prepared in chapter 3 showed the lowest yield of 51%. On the other hand, NiO/AC-ace and Ni/HT showed higher yield of 62% and 60%, respectively. However, high reaction temperature, 423 K, was required in the case of NiO/AC for the yield of 62%. Therefore, NiO/HT can be regarded as the best active catalyst for the oxidation of 1-phenylethanol. In addition, NiO/HT showed good yield of 68% even at 343 K, relatively low temperature, indicating that hydrotalcite is useful as a support of the supported NiO catalyst.

Table 5.3 Comparison of activity among the catalysts prepared in this work

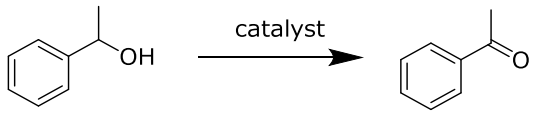

Catalyst	Atmosphere	Temp. (K)	Time (h)	Yield (%)	Chapter
NiO/SiO_2-RT[a]	O_2 1 atm	373	6	51	3
NiO/AC-ace[a]	air 1 atm	423	6	62	4
NiO/HT[b]	O_2 1 atm	373	6	60	5
NiO/HT[b]	air 1 atm	343	10	68	5

1-Phenylethanol: 1 mmol, catalyst: S/C ratio = 12, solvent; [a]*p*-xylene, [b]toluene: 5 mL. S/C ratio is mol ratio of substrate to $catalyst_{Ni}$.

5.3.3. Exploration of the reaction mechanism

The oxidation of 1-phenylethanol using NiO/HT was conducted under various reaction condition in order to reveal the reaction mechanism, and the result is shown in Table 5.4.

NiO/HT showed the catalytic activity also for the oxidation of 1-phenylethanol (Entry 1). NiO and inc-Ni-HT which are bulk compounds of nickel species, hydrotalcite support, and blank test did not produce acetophenone (Entry 2-5). These results indicated that NiO is the active species and NiO needs to be supported on HT for the reaction. In other word, synergy effect of NiO and HT is required for the reaction.

NiO fixed on Al_2O_3, MgO, or SiO_2 resulted in different yield from NiO/HT (Entry 6-8). Basic support such as Al_2O_3 and MgO caused higher yield compared to acidic support such as SiO_2, which indicates that the function as a base support is one of the key factors affecting catalytic activity. Therefore, it can be said that dissociation of O-H by support (namely step iii of Fig. 4.8) is one of the reaction steps, and HT is the most appropriate for the NiO catalysts.

Removing water by molecular sieves and adding water in the reaction system increased and decreased yield, respectively (Entry 9 and 10). This result means that water is produced as a byproduct and it adsorbs on the catalyst, resulting in disturbing the catalytic reaction.

In addition, reaction atmosphere affected the yield. Yield of 44%, 32% and 1.8% was obtained under O_2 1 atm, air 1 atm, and Ar 1 atm, respectively (Entry 1, 11, and 12). Higher pressure of O_2 was favorable for the reaction, but the reaction proceeded to some extent even without O_2 (under Ar atmosphere). This result indicates that acetophenone can be produced even if there is no O_2 molecule, but O_2 is required to regenerate the active site and to obtain more amount of acetophenone.

Table 5.4. Yield of acetophenone for the oxidation of 1-phenylethanol under various reaction condition

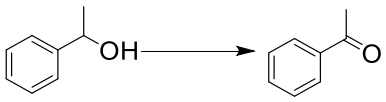

Entry	Catalyst	Yield (%)
1	NiO/HT	32
2	NiO	0.0
3	inc-Ni-HT	0.0
4	Hydrotalcite	0.0
5	blank	0.0
6	NiO/Al_2O_3[a]	15
7	NiO/MgO[a]	12
8	NiO/SiO_2[a]	3.2
9	NiO/HT[b]	39
10	NiO/HT[c]	11
11	NiO/HT[d]	44
12	NiO/HT[e]	1.8

1-Phenylethanol: 1 mmol, catalyst: S/C ratio = 12, toluene: 5 mL, reaction temperature: 343 K, reaction time: 3 h, catalytic reaction was carried out in air. [a]Reaction temperature: 373 K, [b]molecular sieves (0.3 g) was added, [c]distilled water (3 mmol) was added, [d,e]the reaction was carried out in [d]O_2 (1 atm) and [e]Ar (1 atm) atmosphere, respectively. S/C ratio is mol ratio of substrate to $catalyst_{Ni}$.

Based on the above results, a reaction mechanism of 1-phenylethanol oxidation using NiO/HT can be illustrated as shown in Fig. 5.4. In the step i), OH group of 1-phenylethanol adsorbed on NiO site and the reaction started here. Hydrotalcite dissociated O-H bond as a Lewis base and Ni-O bond was formed in step ii). Subsequently, Ni subtracted α-hydride (αC-H) and acetophenone was produced (step iii). Finally, the active site of catalyst surface was regenerated by O_2 molecule in step iv). Small amount of acetophenone can be produced without O_2 since O_2 is not required between step i) and iii), however catalytic cycle does not proceed without O_2 because the active site could not be regenerated if there is no O_2 in the step iv). If without O_2, under Ar atmosphere, the active species cannot be regenerated, resulting in no adsorption of 1-phenylethanol and no dissociation of O-H bond since the active site is occupied by hydrogen.

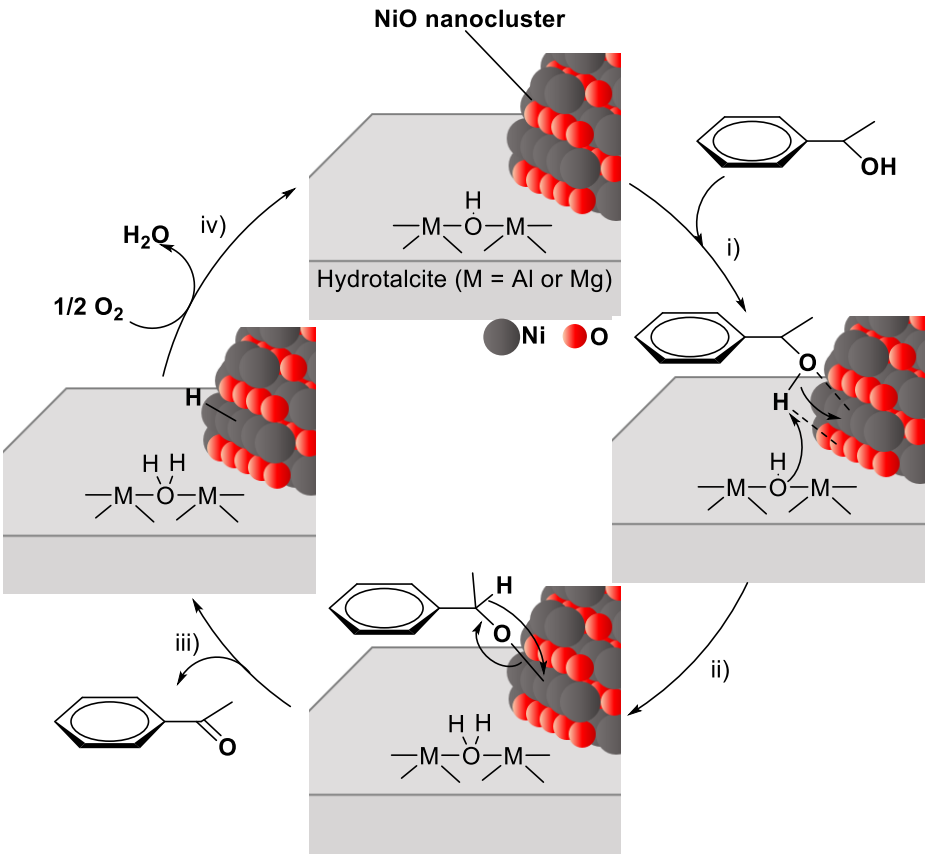

Fig. 5.4. Proposal reaction mechanism for the oxidation of 1-phenylethanol using hydrotalcite supported NiO nanocluster catalyst.

5.4. Conclusion

Supported nickel oxide nanocluster was prepared by using PVP-stabilized nickel colloid as a precursor. Obtained catalysts were applied for the aerobic oxidation of alcohols without additives such as bases, and the catalysts were characterized by XAFS finely.

XAFS measurement revealed the chemical species composing the prepared catalysts including Ni-O-M (M = Al or Mg) structure which is the interfacial structure between nickel oxide nanocluster and hydrotalcite.

NiO/HT catalyst showed the best activity among the catalysts prepared in this work for the oxidation of 1-phenylethanol using O_2 (1 atm) atmosphere without any additives. NiO/HT was more active also compared to the conventional nickel-based catalyst. These results probably were caused by the synergic effect between nickel oxide nanoclusters and supports.

The reaction mechanism was predicted based on the reaction under the different reaction condition. It can be said the reaction occurred on the interface between nickel oxide nanocluster and hydrotalcite support.

Chapter 6

Concluding Remarks

Nickel oxide nanocluster was fixed on the support and applied for the oxidation of alcohols. These catalysts were prepared by utilizing the use of nanocluster and support. The unique property of nanocluster caused by the increase of coordinatively unsaturated site can contribute to the high-catalytic performance. The use of support can contribute to not only the dispersion of active species but also the promoting reactions or appearance of new active site by synergic effect between active species and support. In addition, fixing the nanocluster on the support can enhance the synergic effect due to the increase of interfacial area.

Obtained catalysts were characterized by XAFS, XRD, XPS, and TEM. Particularly analyzing the catalysts by XAFS was strongly focused on in order to clarify the chemical state and local structure of the catalysts for revealing the origin of catalysis. Since XAFS does not need long-ordered structure unlike XRD and it gave this work interesting results and success.

Prepared catalysts were active for the oxidation of alcohols using molecular oxygen without any additives such as base reagents. This is the environmentally friendly catalytic process aiming at the achievement of sustainable society. Moreover, these catalysts were more active compared the conventional nickel-based catalysts although the value of S/C ratio was higher. The promoting effect of the interfacial structure and support led to the enhancement of catalytic activity for the oxidation of alcohols.

Through a series of results obtained in this work, the interfacial mechanism played a great role for the catalytic activity. XAFS and the other characterization revealed that the effective contribution of the support is one of the most important factors for the catalysis of supported catalysts.

In chapter 3, supported NiO nanocluster was prepared by the impregnation method using various nickel precursors.

XAFS found the facts described below; different nickel precursor and support resulted in the different types of nickel species fixed on the support. Not only the types of nickel species but also the size of NiO nanocluster can be controlled by the different precursor, support, and treatment temperature. In particular, in the case of the using $[Ni(NH_3)_6](NO_3)_2$ and SiO_2 as a nickel precursor and a support, respectively, NiO nanocluster and Ni-O-Si structure coexisted as an

active species and an interfacial structure, respectively, on the SiO_2 support.

TEM measurements for NiO(amm)/SiO_2-RT and NiO(ace)/SiO_2-673 revealed that NiO nanocluster that was less than 2 nm mono-dispersed on the support. Determining the cluster size of a catalyst composing plural nickel species by XAFS is difficult because XAFS gives average information. In terms of this problem, TEM was a useful tool to determine to judge if the NiO nanocluster was prepared successfully.

The most interesting result of this chapter is the promoting effect of Ni-O-Si interfacial structure between NiO nanocluster and SiO_2 support. The catalyst composing NiO nanocluster and Ni-O-Si structure showed higher activity for the oxidation of 1-phenylethanol compared to another catalyst composing only NiO nanocluster even if NiO cluster size of the former catalyst was larger than that of the later catalyst. The effective contribution of the interfacial structure resulted in the enhancement of catalysis.

In chapter 4, the supported NiO nanocluster was prepared by using *t*-butoxide-stabilized Ni colloid as a precursor. Catalysis, the role of NiO and support, and the reaction mechanism for oxidation of 1-phenylethanol using supported NiO catalyst consisting of only NiO as a nickel species were discussed.

Interestingly, only activated carbon supported NiO nanocluster was active to the aerobic oxidation of 1-phenylethanol although SiO_2 or Al_2O_3 supported NiO nanocluster were not. Based on the XAFS analysis, there was no great different among these catalysts regarding the kinds of nickel species and NiO cluster size. This result indicates that the support, activated carbon, contributed to the appearance of catalytic activity, it is different from the promoting effect mentioned in chapter 3.

The solvent used at the washing process of catalysts was also important factor which can affect the catalytic activity. The catalysts washed by different solvent was composed of different ratio of NiO and $Ni(OH)_2$. This means that Ni colloid supported on the support transformed into different types of nickel species by different washing solvent because of the high surface activity of small metallic Ni particle.

When the catalysts composed of different ratio of NiO and $Ni(OH)_2$ were used for the oxidation of 1-phenylethanol, the catalyst consisting of higher ratio of NiO showed higher activity. This result indicates that NiO was the active species and that controlling the kinds of nickel species is important for the catalysis.

The reaction mechanism was also proposed based on the results of catalytic reaction under various reaction condition. XAFS revealed that the adsorption of OH group of 1-phenylethanol was the first step of the reaction. This reaction occurred with production of the radical species as an intermediate, and the radical intermediate was produced by subtracting α-hydride (αC-H) on the surface of activated carbon. Since the active species was NiO supported on the activated carbon, the reaction occurred on the interface between NiO nanocluster and activated carbon. We were able to utilize the interfacial structure by supporting the nanocluster on the activated carbon, and the prepared catalyst showed the catalysis for the oxidation of 1-phenylethanol.

In chapter 5, hydrotalcite supported NiO nanocluster catalyst was prepared using PVP-stabilized Ni colloid as a precursor, aiming to create the higher-performance nickel-based catalyst compared to the other catalysts prepared in this work. Promoting the dissociation of O-H bond by hydrotalcite which is a base support was one of the ways to enhance the catalytic activity of supported NiO catalyst for the oxidation of alcohols.

The components of obtained catalyst was found although that catalyst was composed of two types of nickel species by using XAFS analysis. Ni-O-M (M = Al or Mg) which was one of the components was the interfacial structure, the finding the interfacial structure was interesting considering the supported catalysts.

NiO/HT prepared in this chapter showed the highest activity for the oxidation of 1-phenylethanol compared to the other catalysts prepared in chapter 3 and 4. NiO/HT was active also at relatively low reaction temperature, 343 K. It can be said that the combination of nickel oxide and hydrotalcite was favorable for the oxidation of alcohols. Utilizing nanocluster enabled the effective synergic contribution of the support to the reaction.

Reaction mechanism of the alcohol oxidation using NiO/HT was also proposed through

the various results under the different reaction condition. Catalytic cycle was enhanced on the interface of nickel oxide and hydrotalcite, and nanocluster allowed the utilizing synergy effect and dissociation of α-hydride of 1-phenylethanol.

In the all chapters, the oxidation of alcohols occurred on the interface between nickel oxide nanocluster and support. Fig. 6.1 shows the reaction mechanism based on the results obtained in the whole of this work. Subtraction of α-hydride by activated carbon and dissociation of O-H bond by hydrotalcite promoted the catalytic activity of supported NiO nanocluster catalysts for the oxidation of 1-phenylethanol.

The appropriate regulation of the interface structure can enable the appearance of an active site and the promoting effect. Utilizing nanocluster as an active species is also useful to use the interfacial mechanism effectively. If the support and nanocluster could be used effectively, there would be large possibility of the expansion of the science of high-performance catalysts composing nickel or the other base metals.

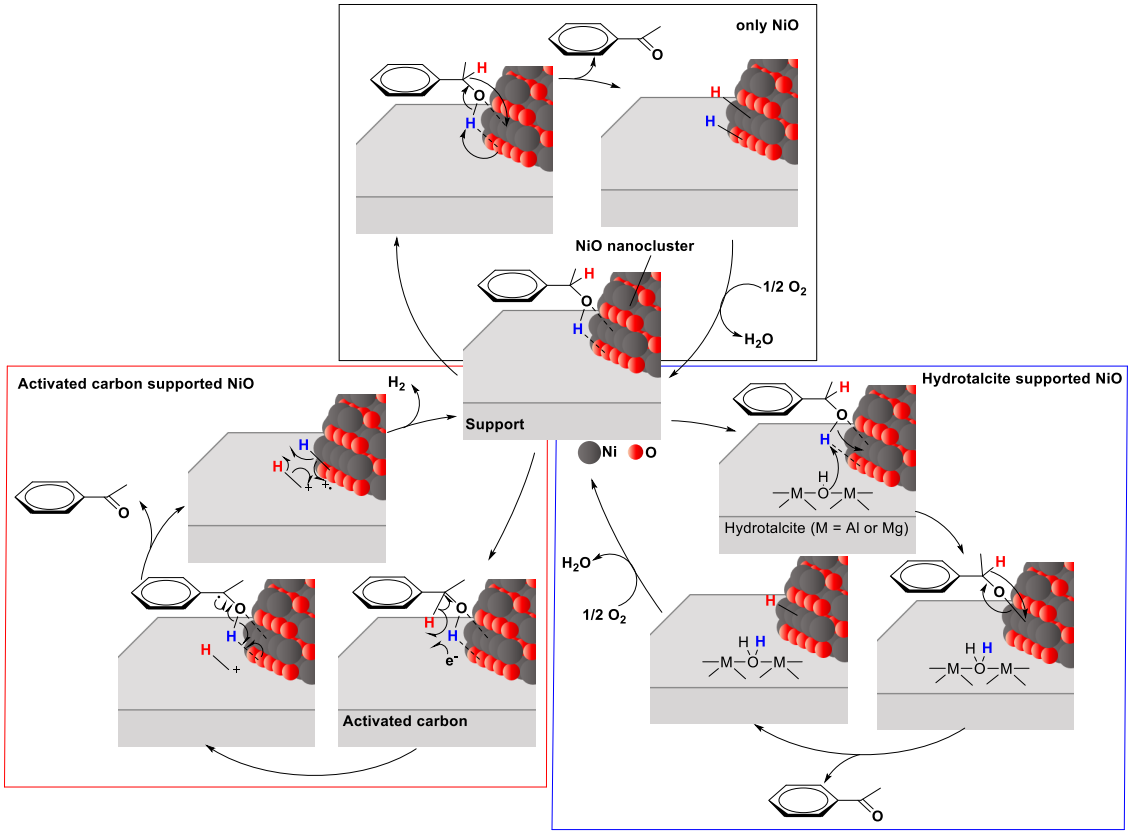

Fig. 6.1. Proposed reaction mechanism of 1-phenylethanol oxidation using supported NiO nanocluster catalysts.

References

[1] E. Kikuchi, K. Segawa, A. Tada, Y. Imizu, H. Hattori, Atarashii Syokubai Kagaku, **2** (2012) 1-8.

[2] T.B. Alexis, *Science*, **299** (2003) 1688-1691.

[3] A.V. Wankhade, G.S. Gaikwad, M.G. Dhonde, N.T. Khaty, S.R. Thakare, *Res. J. Chem. Environ.*, **17** (2013) 84-94.

[4] L.G. Pratibha, D.B. Edward, S. Helveg, P.L. Hansen, G. Suzanne, C.R. Henry, *MRS Bull*., **32** (2007) 1044-1050.

[5] D. Gericke, D. Ott, V.G. Matveeva, E. Sulman, A. Aho, D.Y. Murzin, S. Roggan, L. Danilova, V. Hessel, P. Loeb, D. Kralisch, *RSC Adv.*, **5 (**2015) 15898-15908.

[6] T. Hattori, T. Ida, A. Tsubone, Y. Sawama, Y. Monguchi, H. Sajiki, *Eur. J. Org. Chem.*, **2015** (2015) 2492-2497.

[7] J. Polanski, T. Siudyga, P. Bartczak, M. Kapkowski, W. Ambrozkiewicz, A. Nobid, R. Sitko, J. Klimontko, J. Szade, J. Lelatko, *Appl. Catal. B*, **206** (2017) 16-23.

[8] M.J. Fink, M. Schon, F. Rudroff, M. Schnürch, M.D. Mihovilovic, *ChemCatChem*, **5** (2013) 724-727.

[9] T. Haywood, P.W. Miller, *ChemCatChem*, **6** (2014) 1199-1203.

[10] Y. Wang, Li Yan, C. Li, M. Jian, W. Wang, Y. Ding, *Appl. Catal. A*, **551** (2018) 98-105.

[11] S. Rostamnia, T. Rahmani, H. Xin, *J. Ind. Eng. Chem.*, **32** (3015) 218-224.

[12] M. Bagherzadeh, F. Ashouri, L. Hashemi, A. Morsali, *Inorg. Chem. Commun.*, **44** (2014) 10-14.

[13] N. Linares, C. M.-Marrodan, P. Barbaro, *ChemCatChem*, **8** (2016) 1001-1011.

[14] S. Kataoka, Y. Takeuchi, A. Harada, T. Takagi, Y. Takenaka, N. Fukaya, H. Yasuda, T.

Ohmori, A. Endo, *Appl. Catal. A*, **427-428** (2012) 119-124.

[15] Y. Ma and G. Zhang, *Chem. Eng. J.*, **288** (2016) 70-78.

[16] Y. Liu, Y. Zhang, C. Zhai, X. Li, L. Mao, *Mater. Lett.*, **166** (2016) 16-18.

[17] M. Haruta, *Faraday Discuss.*, **152** (2011) 11-32.

[18] G. Vile, J.P.-Ramírez, *Nanoscale*, **6** (2014) 13476-13482.

[19] A. Philip, J. Lihavainen, M, Keinänen, T.T. Pakkanen, *Appl. Clay Sci.*, **143** (2017) 80-88.

[20] U.S. Geological Survey, Fact Sheet 087-02, http://pubs.usgs.gov/fs/2002/fs087-02/, last modified: May 2005.

[21] M. Viviano, T.N. Glasnov, B. Reichart, G. Tekautz, C.O. Kappe, *Org. Process. Res. Dev.*, **15** (2011) 858-870.

[22] S.T. Martinez, A.C. Pinto, T. Glasnov, C.O. Kappe, *Tetrahedron Lett.*, **55** (2014) 4181-4184.

[23] J. Chen, K. Przyuski, R. Roemmele, R.P. Bakale, *Org. Process Res. Dev.*, **18** (2014) 1427-1433.

[24] D. Gizinski, I. Goszewska, M. Zielinski, D. Lisovytskiy, K. Nikiforov, J. Masternak, M.Z.-Machnik, A. Srebowara, J. Sá, *Catal. Commun*., **98** (2017) 17-21.

[25] Y. Ren, H. Wei, G. Yin, L. Zhang, A. Wang, T. Zhang, *Chem. Commun.*, **53** (2017) 1969-1972.

[26] G. Hahn, J.K. Ewert, C. Denner, D. Tilgner, R. Kempe, *ChemCatChem*, **8** (2016) 2461-2465.

[27] H. Song, T. Wang, X. Jia, Y. Zhu, *j. Alloy. Comp.*, **747** (2018) 523-529.

[28] D.X. Zhang, J. Zhao, Y.Y. Zhang, X.L. Lu, *Int. J. Hydrogen Ener.*, **41** (2016) 11675-11681.

[29] H.P.R. Kannapu, C.A. Mullen, Y. Elkasabi, A.A. Boateng, *Fuel Process Technol.*, **137** (2015) 220-228.

[30] S.B. Ren, H.Z. Wen, X.Z. Cao, Z.C. Wang, Z.P. Lei, C.X. Pan, S.G. Kang, *Chin. J. Catal.*, **35** (2014) 546-552.

[31] D. Baudouin, U. Rodemerck, F. Krumeich, A.D. Mallmann, K.C. Szeto, H. Ménard, L. Veyre, J.P. Candy, P.B. Webb, C. Thieuleux, C. Copéret, *J. Catal*., **297** (2013) 27-34.

[32] S. Wang, G.Q. Lu, *Ind. Eng. Chem. Res.*, **38** (1999) 2615-2625.

[33] M.E. Gálvez, A. Albarazi, P.D. Costa, *Appl. Catal. A*, **504** (2014) 143-150.

[34] X. Li, Q. Hu, Y. Yang, Y. Wang, F. He, *Appl. Catal. A*, **413-414** (2012) 163-169.

[35] P. Kumar, Y. Sun, R.O. Idem, *Energy Fuel*, **21** (2007) 3113-3123.

[36] M.N. Kaydouh, N.E. Hassan, A. Davidson, S. Casale, H.E. Zakhem, P. Massiani, *C. R. Chim.*, **18** (2015) 293-301.

[37] S. Aghamohammadi, M. Haghighi, M. Maleki, N. Rahemi, *Mol. Catal.*, **431** (2017) 39-48.

[38] M.C.J. Bradford, M.A. Vannice, *Appl. Catal. A*, **142** (1996) 73-96.

[39] L. Yao, J. Shi, H. Xu, W. Shen, C. Hu, *Fuel Process Technol.*, **144** (2016) 1-7.

[40] T. Yabe, K. Mitarai, K. Oshima, S. Ogo, Y. Sekine, *Fuel Process Technol.*, **158** (2017) 96-103.

[41] H. Ma, R. Zhang, S. Huang, W. Chen, Q. Shi, *J. Rare Earths*, **30** (2012) 683-690.

[42] J.A. Calles, A. Carrero, A.J. Vizcaíno, M. Lindo, *Schr. Des Forsch. Jülich/Energy Environ.*, **78** (2010) 411-418.

[43] R.T.-Restrup, S. Dahl, A.D. Jensen, *Int. J. Hydrog. Energy*, **39** (2014) 7735-7746.

[44] C. Wu, P.T. Williams, *Appl. Catal. B*, **102** (2011) 251-259.

[45] V. Nichele, M. Signoretto, F. Pinna, F. Menegazzo, I. Rossetti, G. Cruciani, G. Cerrato, A.D. Michele, *Appl. Catal. B*, **150-151** (2014) 12-20.

[46] I. Rossetti, J. Lasso, V. Nichele, M. Signoretto, E. Finocchio, G. Ramis, A.D. Michele, *Appl. Catal. B*, **150-151** (2014) 257-267.

[47] A.D. Michele, A. Dell'Angelo, A. Tripodi, E. Bahadori, F. Sanchez, D. Motta, N. Dimitratos, I. Rossetti, G. Ramis, *Int. J. Hydro. Ener.*, **44** (2019) 952-964.

[48] M.C.S.-Sanchez, R.M. Navarro, I. Espartero, A.A. Ismail, *Top. Catal.*, **56** (2013) 1672-1685.

[49] L.P.R. Profeti, J.A.C. Dias, J.M. Assaf, E.M. Assaf, *J. Power Sources*, **190** (2009) 525-533.

[50] J. R.-Hansen, C.H. Christensen, J. Sehested, S. Helveg, J.R. R.-Nielsen, S. Dahl, *Green. Chem.*, **9** (2007) 1016-1021.

[51] S. Adhikari, S.D. Fernando, S.D.F To, R.M. Bricka, P.H. Steele, A. Haryanto, *Energy Fuels*, **22** (2008) 1220-1226.

[52] V. Nichele, M. Signoretto, F. Menegazzo, A. Gallo, S.V. Dal, G. Cruciani, G. Cerrato, *Appl. Catal. B*, **111-112** (2012) 225-232.

[53] A. Iriondo, V.L. Barrio, J.F. Cambra, P.L. Arias, M.B. Guemez, M.C. S.-Sanchez, R.M. Navarro, J.L.G. Fierro, *Int. J. Hydro. Ener.*, **35** (2010) 11622-11633.

[54] S.M. Kim, S.I. Woo, *ChemSusChem*, **5** (2012) 1513-1522.

[55] A. Iriondo, V.L. Barrio, J.F. Cambra, P.L. Arias, M.B. Güemez, R.M. Navarro, M.C. S.-Sanchez, J.L.G. Fierro, *Catal. Commun.*, **10** (2009) 1275-1278.

[56] A. Iriondo, J.F. Cambra, M.B. Güemez, V.L. Barrio, J. Requies, M.C. S.-Sánchez, R.M. Navarro, *Int. J. Hydrog. Energy*, **37** (2012) 7084-7093.

[57] Z.Y. Huang, C.H. Xu, J. Meng, C.F. Zheng, H.W. Xiao, J. Chen, Y.X. Zhang, *J. Environ. Chem. Eng.*, **2** (2014) 598-604.

[58] A. Iriondo, V.L. Barrio, J.F. Cambra, P.L. Arias, M.B. Güemez, R.M. Navarro, M.C. S.-Sánchez, J.L.G. Fierro, *Top. Catal.*, **49** (2008) 46-58.

[59] I.N. Buffoni, F. Pompeo, G.F. Santori, N.N. Nichio, *Catal. Commun.*, **10** (2009) 1656-1660.

[60] S. Kitamura, T. S.-Enaga, N.O. Ikenaga, T. Miyake, T. Suzuki, *Catal. Lett.*, **141** (2011) 895-905.

[61] L. Tong, A. Iwase, A. Nattestad, U. Bach, M. Weidelener, G. Götz, A. Mishra, P. Bäuerle, R. Amal, G.G. Wallace, A.J. Mozer, *Energy Environ. Sci.*, **5** (2012) 9472-9475.

[62] L. Li, L. Duan, F. Wen, C. Li, M. Wang, A. Hagfeldt, L. Sun, *Chem. Commun.*, **48** (2012)

988-990.

[63] Z. Ji, M. He, Z. Huang, U. Ozkan, Y. Wu, *J. Am. Chem. Soc.*, **135** (2013) 11696-11699.

[64] K. Fan, F. Li, L. Wang, Q. Daniel, E. Gabrielsson, L. Sun, *Phys. Chem. Chem. Phys.*, **16** (2014) 25234-25240.

[65] K.A. Click, D.R. Beauchamp, Z. Huang, W. Chen, Y. Wu, *J. Am. Chem. Soc.*, **138** (2016) 1174-1179.

[66] B. van den Bosch, J.A. Rombouts, R.V.A. Orru, J.N.H. Reek, R.J. Detz, *ChemCatChem*, **8** (2016) 1392-1398.

[67] Y. Gu, Y. Liu, H. Yang, B. Li, Y. An, *Electrochim. Acta.*, **160** (2015) 263-270.

[68] C.W. Kung, Y.H. Cheng, K.C. Ho, *Sens. Actuators. B*, **204** (2014) 159-166.

[69] H. Gao, C. Hao, Y.Q.J. Li, X. Wang, S. Zhou, C. Huang, *J. Alloy. Comp.*, **767** (2018) 1048-1056.

[70] Y. Zhou, C. Sun, X. Yang, G. Zou, H. Wu, S. Xi, *Electrochem. Commun.*, **91** (2018) 66-70.

[71] M.G. Jeong, I.H. Kim, S.W. Han, D.H. Kim and Y.D. Kim, *J. Mol. Catal. A*, **414** (2016) 87-93.

[72] R. Sanchis, D. Delgado, S. Agouram, M.D. Soriano, M.I. Vázquez, E. Rodríguez-Castellónd, B. Solsona, J.M.López Nieto, *Appl. Catal A*, **536** (2017) 18-26.

[73] E.J. Park, J.H. Lee, K.D. Kim, D.H. Kim, M.G. Jeong, Y.D. Kim, *Catal. Today*, **260** (2016) 100-106.

[74] T. Kawabata, Y. Shinozuka, Y. Ohishi, T. Shishido, K. Takai, K. Takehira, *J. Mol. Catal. A*, **236** (2005) 206-215.

[75] W. Zhou, Q. Tao, J. Pan, J. Liu, J. Qian, M. He, Q. Chen, *J. Mol. Catal. A*, **425** (2016) 255-265.

[76] H.-B. Ji, T.-T. Wang, M.-Y. Zhang, Q.-L. Chen, X.-N. Gao, *React. Kinet. Catal. Lett.*, **90** (2007) 251-257.

[77] H. Ji, T. Wang, M. Zhang, Y. She, L. Wang, *Appl. Catal. A*, **282** (2005) 25-30.

[78] N. Sun, X. Zhang, L. Jin, B. Hu, Z. Shen, X. Hu, *Catal. Commun.*, **101** (2017) 5-9.

[79] M. Hudlicky, *Oxidations in organic chemistry*, published by *American Chemical Society*, (1990).

[80] S. Caron, R.W. Dugger, S.G. Ruggeri, J.A. Ragan, D.H.B. Ripin, *Chem. Rev.*, **106** (2006) 2943-2989.

[81] C. Parmeggiani, F. Cardona, *Green Chem.*, **14** (2012) 547-564.

[82] T. Mallat, A. Baiker, *Chem. Rev.*, **104** (2004) 3037-3058.

[83] J. March, Advanced Organic Chemistry: Reactions Mechanisms, and Structure, 4th ed., *John Wiley & Sons, New York*, (1992).

[84] R.A. Sheldon, I. Arends, G.J. Ten Brink, A. Dijksman, *Acc. Chem. Res.*, **35** (2002) 774-781.

[85] R.H. Liu, X.M. Liang, C.Y. Dong, X.Q. Hu, *J. Am. Chem. Soc.*, **126** (2004) 4112-4113.

[86] C.P. Ferraz, M.A.S. Garcia, É. T.-Neto, L.M. Roddi, *RSC Adv.*, **6** (2016) 25279-25285.

[87] M. Gholinejad, M. Afrasi, N. Nikfarjam, C. Nájerac, *Appl. Catal. A*, **563** (2018) 185-195.

[88] J. Albadi, A. Alihosseinzadeh, M. Jalali, M. Shahrezaei, A. Mansournezhad, *Mol. Catal.*, **440** (2017) 133-139.

[89] Y. Hou, X. Ji, G. Liu, Ji. Tang, J. Zheng, Y. Liu, W. Zhang, M. Jia, *Catal. Commun.*, **10** (2009) 1459-1462.

[90] S. A. Majetich, Y. Jin, *Science*, **284** (1999) 470-473.

[91] W. J. Tseng, C.N. Chen, *J. Mater. Sci*., **41** (2006) 1213-1219.

[92] T. Hyeon, *Chem. Commun*., (2003) 927-934.

[93] R. Karmhag, T. Tesfamichael, E. Wäckelgård, G. A. Niklsson, M. Nygren, *Sol. Energy*, **68** (2000) 329-333.

[94] M. Vaseem, N. Tripathy, G. Khang and Y-B. Hahn, *RSC Adv.*, **3** (2013) 9698-9704.

[95] E.V. Panfilova, B.N. Khlebtsov, A.M. Burov, N. G. Khlebtsov, *Colloid J.*, **74** (2012) 99-109.

[96] C. Li, D. Li, G. Wan, J. Xu, W. Hou, *Nanoscale Res. Lett.*, **6** (2011) 440-449.

[97] M. Haruta, T. Kobayashi, H. Sano, N. Yamada, *Chem Lett.*, **16** (1987) 405-408.

[98] H. Kitagawa, N. Ichikuni, S. Xie, T. Tsukuda, T. Hara, S. Shimazu, *e-J. Surf. Sci. Nanotech.*, **10** (2012) 648-650.

[99] H. Kitagawa, N. Ichikuni H. Okuno, T. Hara, S. Shimazu, *Appl. Catal. A*, **478** (2014) 66-70.

[100] N. Ichikuni, O. Tsuchida, J. Naganuma, T. Hara, H. Tsunoyama, T. Tsukuda, S. Shimazu, *Trans. Mat. Res. Soc. Japan*, **37** (2012) 177-180.

[101] T. Sasaki, N. Ichikuni, T. Hara, S. Shimazu, *J. Phys.: Conf. Ser.*, **712** (2016) 012069.

[102] H. Chen, S. He, M. Xu, M. Wei, D.G. Evans, X. Duan, *ACS Catal*., **7** (2017) 2735-2743.

[103] C. Li, H. Kawada, X. Sun, H. Xu, Y. Yoneyama, N. Tsubaki, *ChemCatChem*, **3** (2011) 684-689.

[104] M. Kaur, R. Malhotra, A. Ali, *Renewable Ener.*, **116** (2018) 109-119.

[105] W. Zhang, S. Wang, Y. Zhao, X. Ma, *Fuel Processing Technology*, **178** (2018) 98-103.

[106] J. Wang, C. Liu, J. Qi, J. Li, X. Sun, J. Shen, W. Han, L. Wang, *Environ. Pollution*, **243** (2018) 1068-1077.

[107] Y. Huang, Y. Sun, Z. Xu, M. Luo, C. Zhu, L. Li, *Sci. Total Environ.*, **575** (2017) 50-57.

[108] L. Wang, S. Xu, S. He, F.-S. Xiao, *Nano Today*, **20** (2018) 74-83.

[109] X.-T. Ma, X.-H. Lu, C.-C. Wei, Z.-S. Zhao, H.-J. Zhan, D. Zhou, Q.-H. Xia, *Catal. Commun.*, **67** (2015) 98-102.

[110] A. Singh, L. Spiccia, *Coord. Chem. Rev.*, **257** (2013) 2419-2422.

[111] T. Pietro, P. Alvise, *Chem. Soc. Rev.*, **36** (2007) 532-550.

[112] R.M. David, C. Ming, B.L. Emil, W.C. Geoffrey, *Angew. Chem. Int. Ed.*, **41** (2002) 2599-2602.

[113] Z. Yugen, N.R. Siti, *Chem. Soc. Rev.*, **41** (2012) 2083-2094.

[114] Q.H. Xia, H.Q. Ge, C.P Ye, Z.M Liu, K.X Su, *Chem. Rev.*, **105** (2005) 1603-1662.

[115] T.C. George, C. John, D.H. Katherine, *Int. J. Chem. Eng.*, **2013** (2013) 1-10. Article ID 760915.

[116] A.M. Juan, B.L. Fernando, G. Morales, I. Iglesias, D. Briones, *Energy Fuels*, **23** (2009) 539-547.

[117] B.G Julian, F.I Pilar, M.R Sixto, *J. Sol. Energy Eng.*, **129** (2006) 4-15.

[118] R.R. Debra, *Science*, **299** (2003) 1698-1701.

[119] L. Kesavan, R. Tiruvalam, M.H.A. Rahim, M.I.B. Saiman, D.I. Enache, R.L. Jenkins, N. Dimitratos, J.A. L.-Sanchez, S.H. Taylor, D.W. Knight, C.J. K, G.J. Hutchings, *Science*, **331** (2011) 195-199.

[120] L. Rui, W. Xiqing, Z. Xiang, F. Pingyun, *Carbon*, **46** (2008) 1664-1669.

[121] A.W. Cole, H. Wenyu, T. C.-Kuang, N.K. John, A.S. Gabor, T.F. Dean, *Nat. Chem.*, **2** (2010) 36-41.

[122] S. Kunz, K. Hartl, M. Nesselberger, F.F. Schweinberger, G.H. Kwon, M. Hanzlik, K.J.J. Mayrhofer, U. Heiza, M. Arenz, *Phys. Chem. Chem. Phys.*, **12** (2010) 10288-10291.

[123] D.A. Stevensa, M.T. Hicksc, G.M. Haugenc, J.R. Dahna, *J. Electrochem. Soc.*, **152** (2005) 2309-2315.

[124] H. Heeres, R. Handana, D. Chunai, C.B. Rasrendra, B. Girisuta, H.J. Heeres, *Green Chem.*, **11** (2009) 1247-1255.

[125] L. F.-Xu, W. X.-F, Z. Ying, C. J.-Xiang, *J. Fuel Chem. Technol.*, **46** (2018) 75-83.

[126] S.Z. Abbas, V. Dupont, T. Mahmud, *Int. J. Hydrogen Ener.*, **42** (2017) 2889-2903.

[127] A. Ranjbar, A. Irankhah, S.F. Aghamiri, *J. Environ. Chem, Eng.*, **6** (2018) 4945-4952.

[128] L. Zhang, L. Li , Y. Zhang, Y. Zhao, J. Li, *J. Ener. Chem.* **23** (2014) 66-72.

[129] H. Liua, K. Li, R. Zhang, L. Ling, B. Wang, *Appl. Surf. Sci.*, **426** (2017) 827-832.

[130] S. He, Z. Mei, N. Liu, L. Zhang, J. Lu, X. Li, J. Wang, D. He, Y. Luo, *Int. J. Hydro. Ener.*, **42** (2017) 14429-14438.

[131] X. Wang, L. Zhu, Y. Liu, S. Wang, *Sci. Total Environ.*, **625** (2018) 686-695.

[132] H. Vargas, J.C. Morales, X. Bokhimi, T.E. Klimova, *Catal. Today*, **305** (2018) 133-142.

[133] The Japanese XAFS Society, *Foundations and Applications of XAFS*, (2017).

[134] R. Vanderesse, J.J. Brunet, P. Caubère, *J. Organomet. Chem.*, **264** (1984) 263-271.

[135] T. Sugimoto, X. Zhou, A. Muramatsu, *J. Colloid Interface Sci.*, **259** (2003) 43-52.

[136] I. Yuranov, P. Moeckli, E. Suvorova, P. Buffat, L. K.-Minsker, A. Renken, *J. Mol. Catal. A*, **192** (2003) 239-251.

[137] H. Sarakurai, S. Tsubota, M. Haruta, *Appl. Catal. A*, **102** (1993) 125-136.

[138] R. Narayanan, M.A. E.-Sayaed, *J. Phys. Chem. B*, **109** (2005) 12663-12676.

[139] M.V. Sivaiah, S. Petit, M.F. Beaufort, D. Eyidi, J. Barrault, C. Batiot-Dupeyrat, S. Valange, *Micro. Meso. Mater.*, **140** (2011) 69-80.

[140] T. Lehmann, T. Wolff, C. Hamel, P. Veit, B. Garke, A. S.-Morgenstern, *Micro. Meso. Mater.*, **151** (2012) 113-125.

[141] D.G. Blackmond, E.I. Ko, *Appl. Catal.*, **13** (1984) 49-68.

[142] M. Che, Z.X. Cheng, C. Louis, *J. Am. Chem. Soc.*, **117** (1995) 2008-2018.

[143] A.C. Ferreira, A.M. Ferraria, A.M.B. do Rego, A.P. Gonçalves, M.R. Correia, T.A. Gasche, J.B. Branco, *J. Alloys Compd.*, **489** (2010) 316-323.

[144] J. Luo, H. Yu, H. Wang, H. Wang, F. Peng, *Chem. Eng. J.*, **240** (2014) 434-442.

[145] F. d'Acunzo, P. Baiocco, M. Fabbrini, C. Galli, P. Gentili, *New J. Chem.*, **26** (2002) 1791-1794.

[146] U. Sikander, S. Sufian, M.A. Salam, *J. Hydro. Ener.*, **42** (2017) 19851-19868.

Achievement list

Paper

(1) T. Sasaki, N. Ichikuni, T. Hara, S. Shimazu, Enhancement of Oxidative Dehydrogenation of Alcohols by Utilizing Hydrotalcite as Support of NiO Nanocluster Catalyst, *Chem. Lett.*, in press (doi: 10.1246/cl.181040). **[Chapter 5]**

(2) T. Sasaki, F. Devred, P. Eloy, E.M. Gaigneaux, T. Hara, S. Shimazu, N. Ichikuni, Development of supported NiO nanocluster for aerobic oxidation of 1-phenylethanol and elucidation of reaction mechanism via X-ray analysis, *BCSJ*, in press (doi:10.1246/bcsj.20180387). **[Chapter 4]**

(3) T. Sasaki, N. Ichikuni, T. Hara, S. Shimazu, Study on the promoting effect of nickel silicate for 1-phenylethanol oxidation on supported NiO nanocluster catalysts, *Catal. Today*, **307** (2018) 29-34. **[Chapter 3]**

(4) T. Sasaki, N. Ichikuni, T. Hara, S. Shimazu, Structural analysis of NiO nanocluster catalysts on SiO_2 by using XAFS measurements, *J. Phys.: Conf. Ser.*, **712**, (2016) 012069. [Not included]

(5) H. Sudrajat, Y. Zhou, T. Sasaki, N. Ichikuni, H. Onishi, *Phys. Chem. Chem. Phys.*, in press. [Not included]

(6) L. An, T. Sasaki, P.G. Weidler, C. Wöll, N. Ichikuni, H. Onishi, Local Environment of Strontium Cations Activating $NaTaO_3$ Photocatalysts, *ACS Catal.*, **8** (2017) 880-885. [Not included]

Presentation at the international conference

[Oral]

(1) ◯T. Sasaki, N. Ichikuni, T. Hara, S. Shimazu, Study on the promoting effect of nickel silicate for 1-phenylethanol oxidation on supported NiO nanocluster catalysts, 9th International Conference on Environmental Conference (9th ICEC 2016) (Paper#191) Newcastle (Australia), July・2016. **[Chapter 3]**

[Poster]

(1) ◯T. Sasaki, N. Ichikuni, T. Hara, S. Shimazu, Study on the effect of the interfacial structure of supported NiO nanocluster catalysts to 1-phenylethanol oxidation reaction, 17th International Conference on X-ray Absorption Fine Structure (XAFS2018) (#61, IX-46) Kraków (Poland), 22-27, July 2018. **[Chapter 4]**

(2) ◯T. Sasaki, N. Ichikuni, T. Hara, S. Shimazu, Construction of a clean process with colloid derived NiO nanocluster catalysts for oxidation of 1-phenylethanol, 19th International Sol-Gel Conference (P151) Liege (Belgium), September 2017. **[Chapter 4]**

(3) ◯T. Sasaki, N. Ichikuni, T. Hara, S. Shimazu, Interfacial structure of SiO_2 supported NiO nanocluster and its promoting effect for 1-phenylethanol, 2nd Joint Workshop on Chirality in Chiba University (WCCU) and on Soft-Molecule Activation (STA), Chiba (Japan), December 2016 **[Chapter 3]**

(4) ◯T. Sasaki, N. Ichikuni, T. Hara, S. Shimazu, The support effect of NiO nanocluster catalysts on thiophenol coupling reaction, Joint Workshop on Chirality in Chiba University (WCCU) and on Soft-Molecule Activation (STA), Chiba (Japan) 17th March 2016. [Not included]

(5) ◯T. Sasaki, N. Ichikuni, T. Hara, S. Shimazu, Structural analysis of NiO nanocluster catalysts on SiO_2 by using XAFS measurements, 16th International Conference on X-ray Absorption Fine Structure (XAFS16), (IV_Tue_14), 23rd-28th August 2015, Karlsruhe, Germany. [Not included]

Presentation at the domestic conference

[Oral]

(1) ◯佐々木拓朗・一國伸之・原孝佳・島津省吾，アルコール酸化反応に有効な酸化ニッケルナノクラスターの活性起源に関する研究, 第 21 回 XAFS 討論会（O102）（札幌），9・2018 **[Chapter 5]**

(2) ◯佐々木拓朗・一國伸之・原孝佳・島津省吾，PVP 保護ニッケルコロイドを用いた 1-フェニルエタノール酸化反応に有効な酸化ニッケルナノクラスターの開発，第 122 回触媒討論会（1H20）（函館），9・2018（口頭）**[Chapter 5]**

(3) ◯佐々木拓朗・一國伸之・原孝佳・島津省吾，1-フェニルエタノール酸化反応に有効な担持 NiO ナノクラスター触媒の表面化学種の解析，第 20 回 XAFS 討論会（5-05）（姫路），8・2017 **[Chapter 4]**

(4) ◯佐々木拓朗・一國伸之・原孝佳・島津省吾，金属コロイドを前駆体とした担持 NiO ナノクラスターの構築と構造解析，日本化学会 第 97 春季年会（4A8-11）（日吉），3・2017 **[Chapter 4]**

(5) ◯佐々木拓朗・一國伸之・原孝佳・島津省吾，NiO ナノ粒子と担体との界面構造の分析とプロモ―ティング効果，第 19 回 XAFS 討論会 (4-01) (名古屋)，9・2016 学生奨励賞受賞 **[Chapter 3]**

(6) ◯佐々木拓朗・一國伸之・原孝佳・島津省吾，担持型 NiO ナノクラスター触媒の調製と 1-フェニルエタノール酸化反応への応用，第 118 回触媒討論会 (1D12) (盛岡) 2016.9.21 **[Chapter 3]**

(7) ◯佐々木拓朗・一國伸之・原孝佳・島津省吾, 1-フェニルエタノールの酸化反応に有効な担持 NiO ナノクラスターの活性構造に関する研究，第 116 回触媒討論会 (3F13) (津) 2015.9.18 **[Chapter 3]**

(8) ◯佐々木拓朗・一國伸之・原孝佳・島津省吾，担持 NiO ナノクラスターのチオフェノールカップリング反応に対するナノサイズ効果と XAFS による構造解析，第 95 回日本化学会春季年会 (1F8-33) (船橋), 2015.3.26 [Not included]

(9) ◯佐々木拓朗・一國伸之・原孝佳・島津省吾,シリカ担持ニッケル触媒によるチオフェノールカップリング反応の粒径依存に関する研究,第 114 回触媒討論会 (2G01) (東広島), 2014.9.26 [Not included]

[Poster]

(1) ◯佐々木拓朗・一國伸之・原孝佳・島津省吾，金属コロイドを前駆体とした担持 NiO ナノクラスターの局所構造に関する研究，2016 年度量子ビームサイエンスフェスタ（つくば）2017.3.16 **[Chapter 4]**

(2) ◯佐々木拓朗・一國伸之・原孝佳・島津省吾，SiO_2 担持 NiO ナノクラスター触媒における担体界面構造に関する研究，XAFS 夏の学校 2016（小樽）2016.9.26 **[Chapter 3]**

(3) ◯一國伸之・佐々木拓朗・小川雅裕・原孝佳・島津省吾,XAFS を用いた鉄鋼スラグ中の Mg 種の分析，第 18 回 XAFS 討論会 (2P10) (つくば), 2015.7.30 [Not included]

(4) ◯佐々木拓朗・一國伸之・原孝佳・島津省吾, XAFS による担持 NiO ナノクラスターおよび担体界面の構造解析,第 3 回物構研サイエンスフェスタ (138H) (つくば), 2015.3.17 [Not included]

(5) ◯佐々木拓朗・一國伸之・原孝孝佳・島津省吾,保護基フリーの NiO ナノクラスター触媒が示すナノサイズ効果,第 4 回 CSJ 化学フェスタ (P8-100) (東京), 2014.10.16 [Not included]

(6) ◯佐々木拓朗・一國伸之・土田理・原孝佳・島津省吾，NiO ナノクラスター触媒のサイズ精密制御への試み, XAFS 夏の学校 2013, (P12) (草津町), 2013.8.29 [Not included]

Award

(1) 学生奨励賞受賞

◯佐々木拓朗・一國伸之・原孝佳・島津省吾，NiO ナノ粒子と担体との界面構造の分析とプロモ―ティング効果，第 19 回 XAFS 討論会 (4-01) (名古屋)，9・2016 **[Chapter 3]**